NTNU – Trondheim
Norwegian University of
Science and Technology

Neutron Stars

The electromagnetic forces at the surface
and its implications.

Nicolas Vallet Sogge

Physics
Submission date: May 2013
Supervisor: Jan Myrheim, IFY

Norwegian University of Science and Technology
Department of Physics

Acknowledgments

I would like to thank my supervisor, professor Jan Myrheim, who accepted me as his master student and guided me along the course of this thesis, whilst also being lecturer in several of the courses I have taken. My friends and colleagues at the study room B3-131 with whom I have had a lot of physical and nonphysical discussions have been important to me, giving inspiration and distractions. My time spent at NTNU would not have been the same without my friends, who made me feel like I belong here.

This work is dedicated to you.

Abstract

This thesis is the fruit of the master degree. An open question regarding the electromagnetic forces on a neutron star is the foundation. The electromagnetic forces are strong on a neutron star, yet they seem to be neglected compared to the force of gravity when describing the star. Neutron stars are assumed to have a very spherical shape, but if the electromagnetic forces cannot be neglected, could the shape be transformed? Being outside the area of expertise of my supervisor, the task became very exploratory, trying to get an understanding of what neutron stars are. Using a simple model for the magnetic field, an oscillating magnetic dipole, the forces on a test particle at the surface of the star was found. Using the values found the next challenge is to find the charge distribution giving rise to the strong electromagnetic fields. Due to the open and vague problematic and time lost on technical difficulties with the simulations the results found in this thesis are limited. The work done may open for the possibility of future work within the subject as neutron stars has become familiar to the graduate student.

Sammendrag

Denne oppgaven er avslutningen på en masteroppgave. Motivasjonen bak oppgaven lå i de elektromagnetiske kreftene i en nøytronstjerne. Disse kreftene kan bli veldig sterke. Likevel blir disse neglisjert i forhold til de gravitasjonelle kreftene. Hensikten med oppgaven var å finne ut i om dette var forsvarlig. I og med at nøytronstjerner er utenfor fagområdet til min veileder ble oppgaven en utforskningsoppgave, både for studenten og for veilederen, samt veldig vagt definert. Ved å lage en enkel modell på magnetfeltet, en oscillerende dipol, regner oppgaven påkreftene påladede partikler på overflaten. Etter å ha funnet feltet på overflaten var målet å regne ut ladningsfordelingen. Denne oppgaven viste seg å bli vanskelig, med tekniske problemer med programeringa samt en ulœselig ligning. Sammen med den utforskende og vage naturen til oppgaven medførte dette til en resultatmessig begrenset avhandling. Til gjengjeld har arbeidet utført tillatt studenten å bli godt kjent med nøytronstjerner, som kan åpne veier for fremtidig arbeid i det fagfeltet.

Table of Contents

List of Figures

Abbreviations

EoS	=	Equation of state
SNR	=	Supernova remnant
NS	=	Neutron star
GR	=	General relativity
SR	=	Special relativity
SGR	=	Soft gamma ray
GRB	=	Gamma ray burst
LMXRB	=	Low mass X-ray binary
IMXRB	=	Intermediate mass X-ray binary
HMXRB	=	High mass X-ray binary
AMXRB	=	Accreting millisecond X-ray binary
PSR	=	Pulsar
TOV	=	Tolman-Oppenheimer-Volkof

Introduction

A neutron star is a compact object formed in a core-collapse supernova explosion or in an accretion process of a white dwarf. Its radius is of the order of tens of kilometers and its mass on the order of one solar mass. These values indicate an extremely dense composition. The innermost matter can reach values significantly exceeding the atomic nuclei density. The gravitational energy reaches 20% of the rest mass energy. Neutron stars also exhibit enormous angular momentum and electromagnetic fields. Such conditions are unavailable on Earth, hence neutron stars are unique laboratories to test theories of gravity in the strong field regime. Binary systems composed of neutron stars or black holes may be the source of new physics in the emission of gravitational waves. In other words, neutron stars are excellent subjects for unveiling more about the physical laws in nature. This paper will give a brief introduction to neutron stars, with the physics present in such compact objects and look at the electromagnetic field and its implication on charges.

Chapter 1

An introduction to Neutron Stars

1.1 A historical discovery

Two years after the discovery of the neutron[1], the possibility of a compact star predominantly made out of neutrons as resulting core of a *supernova*, defined in section 1.2.2, was postulated by Walter Baade and Fritz Zwicky in 1934. According to their hypothesis, all the neutrons would fall down to the center of the star due to the strong gravitational force. However, due to the small size and therefore highly unlikely detection, the neutron star model was not pursued for decades. This changed dramatically in 1967, thanks to the serendipity and the diligence of an Irish graduate student by the name of Jocelyn Bell. Bell and her advisor, Anthony Hewish, were working on radio observations of quasars, which had been discovered in 1963. Bell and her fellow graduate students had constructed a scintillation array for the observations. She went on to analyze the charts of data produced. One day she noticed a bit of "scruff" that appeared on the charts every second and a third. The scruff was so regular that she first thought it must be artificial. However, careful checking showed that indeed the signal was extraterrestrial, and in fact that it must be from outside the solar system. This source, CP 1919, named a *pulsar* for its radio pulses, was the first to be discovered[2].

The discovery initiated a storm of activity that has still not abated. A number of other pulsars were discovered, including one in the Crab Nebula, site of a famous supernova in the year 1054 that was observed by Chinese, Arabic, and North American-astronomers[3]. Within a year or so of the initial discovery, it became clear that:

- pulsars are fast, with periods known in 1968 from 0.033 seconds: the Crab pulsar, to about 2 seconds,

[1]Discovered in 1932 by James Chadwick, which earned him the Nobel Prize in Physics in 1935.

[2]In 1974, A. Hewish was awarded the Nobel Prize "for his decisive role in the discovery of pulsars", without J. Bell. Bell was a critical part in the system yet did not participate in the award, which led to the saying "no-Bell prize".

[3]But not recorded by Europeans.

- the pulsations are very regular, with a typical rate of change of only a second per ten million years,
- over time, the period of a pulsar always increases slightly.

With this data, it was realized quickly that pulsars had to be rotating neutron stars. With certain exceptions that do not apply in this case, if a source varies over some time t, then its size must be less than the distance light can travel in that time, or ct (otherwise the variation would be happening faster than the speed of light). Thus, these objects had to be less than 300 000 km/s times 0.033 seconds, or 10 000 km, in size. This restricts us to white dwarfs, neutron stars, or black holes. A periodic signal from such objects can be achieved via pulsation, rotation, or a binary orbit. White dwarfs are large enough that their maximum pulsational, rotational, or orbital frequencies are more than a second, so this is ruled out. Black holes do not have solid surfaces to which to attach a beacon, so rotation or vibration of black holes is eliminated. Black holes or neutron stars in a binary could produce the required range of periods, but the binary would emit gravitational radiation, the stars would get closer together, hence the period would decrease, not increase. Pulsations of neutron stars typically have periods of milliseconds, not seconds. The only thing left is rotating neutron stars, and this fits all of the observations admirably.

There have now been more than 1000 pulsars discovered, with periods from about 1.4 milliseconds to more than 5 seconds. Their discovery is considered one of the three most important astronomical discoveries in the latter half of the twentieth century[4]. Neutron stars show a wide variation of characteristics, divided into different categories :

- radio pulsars, explained in section 2.1,
- accreting X-ray pulsars, explained in section 2.2,
- rotating radio transients(RRTs), a pulsar which emits short moderately bright radio pulses, which will not be explained,
- magnetars, explained in section 2.3,
- isolated neutron stars, briefly explained in section 1.2.2.

Theoretical stellar evolution models combined with observational population studies indicate the existence of $10^8 - 10^9$ neutron stars in the Milky Way.

1.2 The birth of a neutron star

1.2.1 The association between pulsar and supernova remnant

The leading theory explaining the creation of neutron stars is the core collapse leading to a supernova. However, this implies a reliable association between a pulsar and a SNR, which requires a similarity between ages and location[5]. Two cases were quickly found: the Crab pulsar and Vela pulsar were quickly associated with their respective supernova remnant.

[4] Along with quasars and the microwave background.
[5] Another source is the collapse of an accreting white dwarf.

But it would take another 14 years to find a new pair. Searches were made inside known SNRs for radio pulsars, but produced no positive result in spite of the growing number of known pulsars found in surveys. In 1982 (PSR 1509-58, Seward & Harden) and 1984 (PSR 0540-69, Seward *et al.*) two new pulsating sources were detected in SNRs using the *Einstein Observatory*. PSR 1509-58 was immediately identified as a radio pulsar, with the highest spin down rate $\dot{P}$ known at the time. However, PSR 0540-69 could at first only be studied through X-rays and optical wavelengths. Its radio detection came in 1993, making it a radio quiet pulsar for ten years.

The different lifetimes is part of the reason SNR-PSR pairs are not often observed. SNRs emit radiation for several thousands of years, while neutron stars are active for millions. Another reason, pulsar kicks, will be explained in section 1.2.2.

1.2.2 The supernova process

During the fusion process in a star, heavier and heavier elements fuse together until reaching iron and nickel, where no energy is released when fused. The star separates into different layers dominated by an element, increasing in mass when going further into the star, with hydrogen and helium at the surface and iron and nickel in the core. The core becomes bigger, heavier and more compact as time goes on. The gravity is supported by electron degeneracy pressure. If the star has a mass between $8M_{\odot}$ and 20-30$M_{\odot}$[6] the core reaches the *Chandrasekhar limit*[6][7] of $1.44M_{\odot}$, having a radius of $\sim 10^6$ m, becoming too compact to support the pressure and collapse, leading to an implosion. During the collapse the fall velocity will reach up to 23% of the light velocity, generating temperatures up to 10^{11}K. In the core the threshold for inverse β-decay is reached, creating neutrons and neutrinos in large amounts:

$$e^- + p \rightarrow n + \nu_e$$

Approximately 99% of the radiated energy is radiated through neutrinos, corresponding to $3.0 \cdot 10^{46}$ J. The total number of 10^{58} neutrinos were radiated in the supernova SN1987A. Even though neutrinos have such a small probability to react, having a mean free path in lead of half a light year, the enormous amount is able to exert a massive force on the falling matter. The core will become very rich in neutrons and the combination of neutron degeneracy pressure and neutrino wind will be able to stop the collapse. If the star mass is above the treshold of 20-30 $M_{\odot}$, the core will surpass the *Tolman-Oppenheimer-Volkoff limit*[8], the neutron degeneracy pressure will not be able to stop and support the pressure. The star will then collapse even further to an exotic star as mentioned earlier or a black hole. The degeneracy pressure and the massive neutrino wind will in turn be able to repel and push away all the infalling matter leading them to be shot from the star and creating a massive explosion, a *supernova*. The core survives the supernova, inheriting most of the magnetic field and angular momentum of the progenitor star. The expelled

[6]The upper limit depends on the EoS and is much more uncertain than the lower limit. Stars with lower mass burn out and become white dwarfs, and stars with higher mass become black holes or postulated, but unseen, stars like quark star, strange stars etc...

[7]The maximum mass for a stable core supported by electrons.

[8]The maximum mass for a stable core supported by neutrons[6].

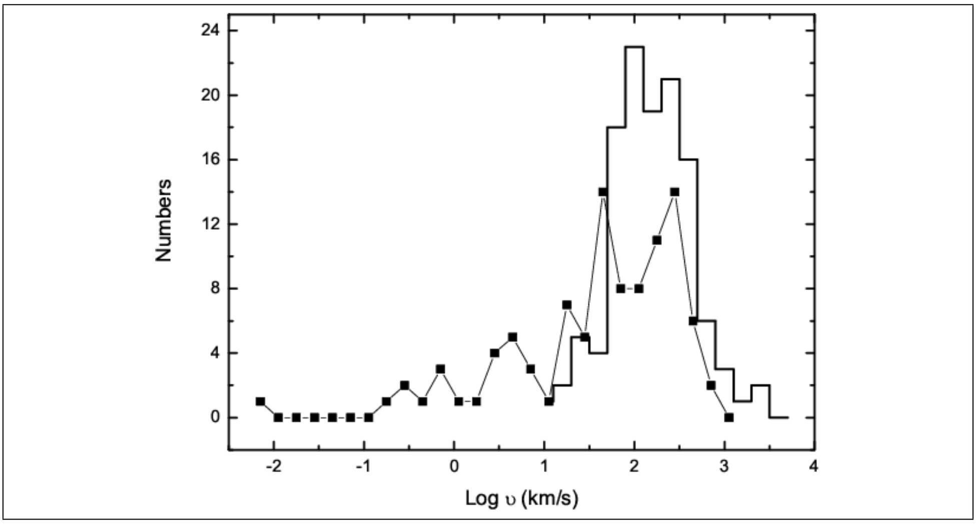

Figure 1.1: Pulsar kick velocities: The distribution of the pulsar's kick velocity and that derived from a theoretical model. The solid step line is the observed kick distribution. The line with squares is the modeled kick distribution derived from the theoretical model. Graph taken from *Astronomy and Astrophysics*[7].

matter will create a visible halo which is called the *supernova remnant*. During the exploding part of the process, the matter may not be isotropically distributed. This will give the neutron star momentum which can reach high values. As indicated by figure 1.1 the velocities can reach above 1000 km s^{-1}. With such kick velocities the pulsar can escape the SNR, as illustrated in figure 1.2, whose expansion is slowed down by the interstellar medium, and even the galaxy itself. Neutron stars which have been ejected away from other mass concentrations become isolated neutron stars. The high velocity is one of the reasons pulsars are found without their corresponding SNRs.

The supernova process is a complicated, and not yet fully understood concept. For further details one has to go in more profound articles and books than the one used here[6], which is more of an introduction, but enough for this thesis.

1.2.3 The connection between the neutron star and the SNR

SNRs are visible, indicating that they radiate energy. Indeed, the radiation corresponds to *synchrotron radiation*, charged particles in motion radiating in the presence of magnetic fields and the cooling of the hot relativistic matter. When colliding with the interstellar matter, the shock front heats up, fueling the thermal radiation at the cost of its velocity. The SNR can expand over tens of parsecs before its speed falls below the local sound speed. The radiation from the nebula is partially powered by magnetic fields. These fields can be weak interstellar magnetic fields, and the more powerful magnetic field of the neutron star, core of the same progenitor star as the SNR. This energy transfer slows the pulsar in the SNR down, explaining why their spin down rate is stronger than for isolated neutron stars, which were shot out of the nebula.

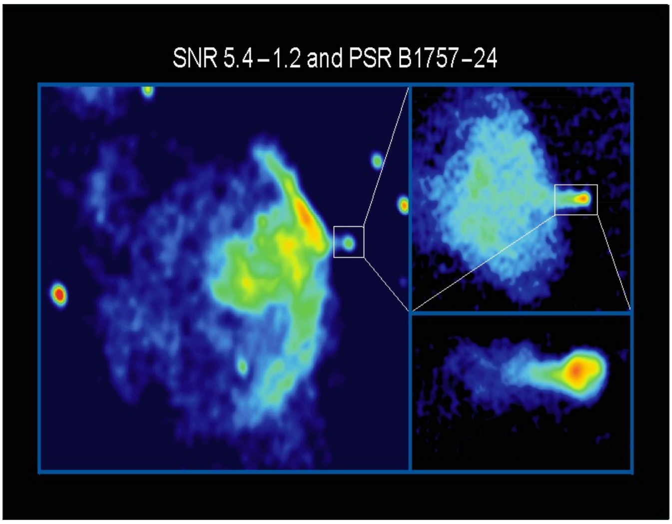

Figure 1.2: A SNR with a pulsar, where the pulsar has been ejected out of the SNR. The SNR as seen as the disc, with very radiating extremity near the pulsar which is fueled by the pulsar's magnetic field. The pulsar is the escaping source to the right, being zoomed at. Image taken from *Nature*[9].

1.3 The interior

The interior of the neutron star is separated into three main regions: an outer layer of plasma, called the *atmosphere*, a thick envelope with the mixture of atomic nuclei and free neutrons, protons and electrons, called the *crust* and an inner region of ultra dense matter which composition is unknown, called the *core*. The crust and core can be separated into subregions, an inner and an outer layer as illustrated by figure 1.3. The atmosphere is very thin, with thickness from several millimeters to several ten centimeters, depending on the surface temperature. The hotter the surface the thicker the atmosphere. Most of the radiation is emitted from the atmosphere. The top of the crust, with a thickness of a few hundred meters, consists mainly of iron 56 ions and free electrons. The electrons are non-degenerate in this layer, and become increasingly degenerate and ultra-relativistic with increasing depth. Going deeper into the star the pressure is enough to rise the equilibrium atomic weights so one might find very neutron rich elements such as Z=40, A=120, which are nonexistent on earth and very unstable in more ordinary conditions. At densities of 10^6 g$\cdot$cm^{-3} the electrons become noticeably degenerate, meaning that electrical and thermal conductivities are huge since the electrons can travel great distances before interacting.

Deeper yet, at the bottom of the outer crust, corresponding to densities around 4×10^{11} g$\cdot$cm^{-3}, the *neutron drip* layer is reached. At this layer, it becomes energetically favorable for neutrons to float out of the nuclei and move freely around: the electron Fermi energy becomes high enough to allow inverse β-decay, so the neutrons "drip" out. Even further down, the neutrons are mainly free, with a $5\% - 10\%$ sprinkling of protons and electrons. The Fermi energy of the electrons also allows μ production. As the density increases, a phase known as the *pasta-antipasta*[12] sequence appears. At relatively low (about 10^{12} g·cm^{-3}) densities, the nucleons are spread out like meatballs[9] that are relatively far from each other. At higher densities, the nucleons merge to form spaghetti-like strands, and at even higher densities the nucleons look like sheets (such as lasagna). Increasing the density further brings a reversal of the above sequence, where mainly nucleons are present, but the holes form (in order of increasing density) anti-lasagna, anti-spaghetti, and anti-meatballs, also called *Swiss cheese*. Going even deeper, where the density exceeds the nuclear density 2.8×10^{14} g·cm^{-3} by a factor of 2 or 3, exotic matter might form, like pion condensates, lambda hyperons, delta isobars, and quark-gluon plasmas. These densities are not available in the laboratory and therefore our knowledge is greatly restricted. Different hypothesis exist, in form of the relation between density, pressure and temperature $P(\rho, T)$, called the *equation of state*. The EoS is the key element that sets a limit on the range of possible masses to a neutron star and describes its composition. EoS' are a complicated subject and will not be further explained.

1.4 Spin history

Neutron stars rotate very rapidly, up to 600 times per second. A major question is how they spin when they are born. They may be born rotating very fast, with periods comparable to a millisecond, although evidence is ambiguous. They will then spin down due to magnetic torques. This seems to be supported by the fact that some of the youngest pulsars, such as the Crab pulsar (33 ms) and the Vela pulsar (80 ms) have unusually short periods. After a pulsar is born, its magnetic field will exert a torque and slow it down, with typical spin down rates of 10^{-13} s/s for a young pulsar like the Crab.

Although the overall tendency is for isolated pulsars to slow down, they can undergo very brief periods of spin-up. These events are called *glitches*, and they can momentarily change the period of a pulsar by up to a few parts in a million. The effects of glitches decay away in a few days, and then the pulsar resumes its normal spin down. In current models of glitches, the superfluid core and solid crust are presumed to couple impulsively, and since the crust is spun down by the magnetic field while the superfluid keeps rotating at its original rate, this coupling speeds up the crust, leading to the observed spin-up. It is very difficult to treat this process from first nuclear principles, because the critical angular velocity difference at which the crust and superfluid finally couple depends sensitively on various ill-determined properties of neutron superfluids. Since these properties are not directly accessible by experiments the current phenomenological description is the best available. Incidentally, the glitch also heats up the crust, and late in the lifetime of the neutron star, heating by rotational dissipation can actually become a significant source of heat and affect the temperature evolution.

Assuming the most of the angular momentum is conserved in the transition to neutron star one can find the crude relation between periods:

The angular momentum is defined as:

$$I_i \omega_i = I_f \omega_f,$$

[9] Using the food language.

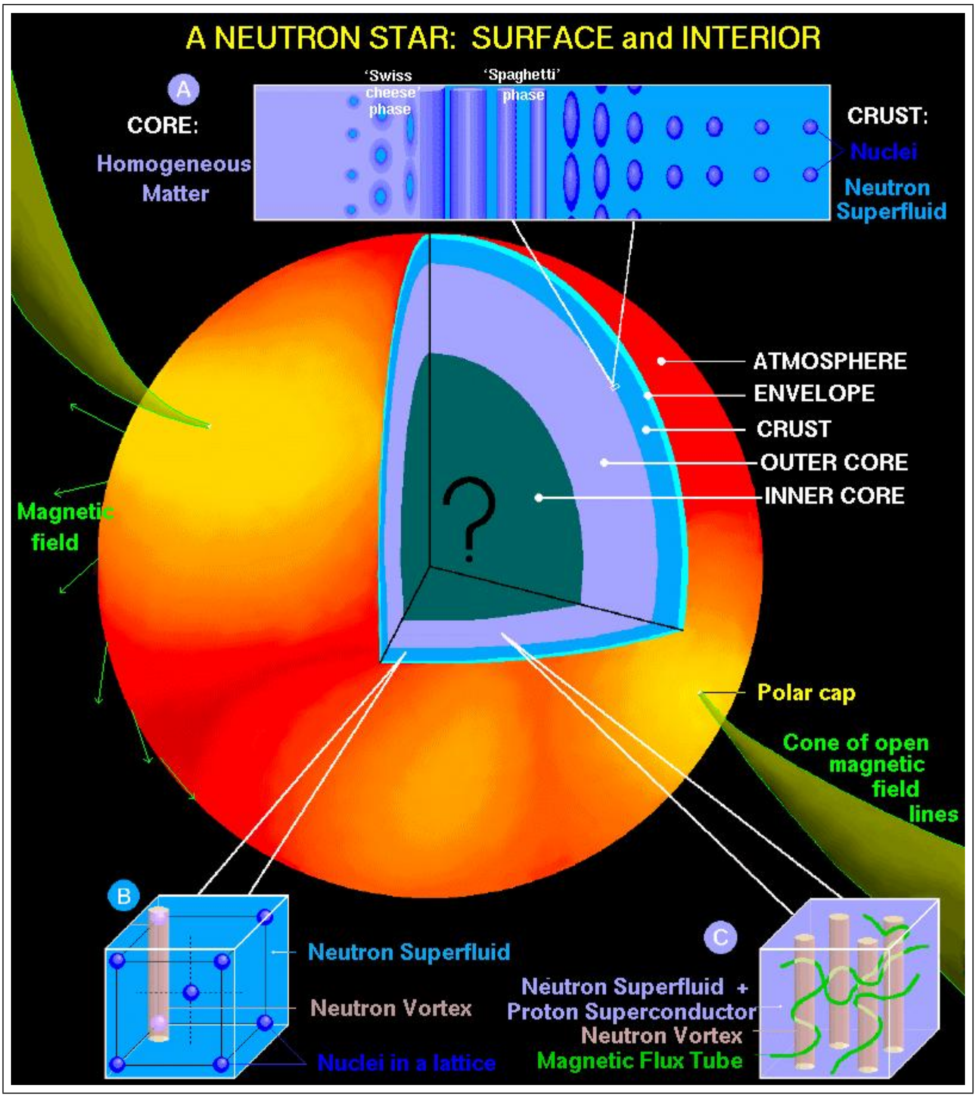

Figure 1.3: Neutron star structure showing the interior[14].

$$CM_iR_i^2\omega_i = CM_fR_f^2\omega_f.$$

Moment of inertia for a sphere: $I = CMR^2$. The C factor depends on the mass distribution in the sphere. ω is the rotational frequency.

$$\omega_f = \omega_i\left(\frac{R_i}{R_f}\right)^2.$$

In terms of the rotation period P, this is:

$$P_f = P_i\left(\frac{R_f}{R_i}\right)^2.$$

In the case of an iron core collapsing to form a neutron star the period becomes P_f. This relation is more accurate in the case where a white dwarf accretes enough matter to collapse into a neutron star.

$$P_{NS} \approx 3.8\times10^{-6}P_{core}, \tag{1.1}$$

where P_{core} is the rotational period of the core. The question of how fast the progenitor core may be rotating is difficult to answer. As a star evolves, its contracting core is not completely isolated from the surrounding envelope, so one cannot use the simple approach to conservation of angular momentum described above. For purposes of estimation, the observed rotation period for the white dwarf 40 Eridani B, P_{core}=1350s, is chosen. Inserting this into equation 1.1 results in a rotation period of about 5×10^{-3}s. Thus neutron stars rotate very rapidly when they are formed, with rotation periods on the order of a few milliseconds.

Using the formula for electron degeneracy and switching the electron mass with the neutron mass one gets the neutron star radius:

$$R_{NS} \approx \frac{(18\pi)^{2/3}}{10}\frac{\hbar^2}{GM_{NS}^{1/3}}\left(\frac{1}{m_H}\right)^{8/3}. \tag{1.2}$$

Where m_H is the mass of hydrogen[6]. A typical neutron star mass is $1.4M_\odot$, which according to the formula equation 1.2 will have a radius of 4400m. However, more advanced models show a typical radius larger by a factor of three.

Such a combination between mass and radius results in an incredibly compact star with an average density of 6.65×10^{17}kg·m^{-3}, which is greater than the typical density of an atomic nucleus, $\rho_{nucleus} \approx 2.3\times10^{17}$ kg·m^{-3}.

Chapter 2

Evolution of neutron stars

As seen in the calculations above, a young neutron star will have a high rotational frequency of the order of 10^{-2} s^{-1}. Two different paths exist. In some cases the angular momentum will be transformed into magnetic energy through a dynamo effect. The resulting star will have a very strong magnetic field of the order of 10^8 T and a period of the order of 10^0 s. In the other, but most common one, the neutron star will slowly lose angular momentum through meridional currents. It will become a typical *radio pulsar*. The frequency of the observed pulsars range from 1.4 ms to 5 s, gradually slowing down. A general connection between age and period exists: the longer period, the older the star. Below a certain frequency they are no longer observable and they end in the *graveyard* phase of the neutron star life cycle. For most neutron stars this is the end. However, some wake up from their grave.

2.1 Radio pulsars

Radio pulsar is the most common form of neutron star, with a population exceeding 1700 objects out of 2000 known neutron stars. Realistic estimations predict a total galactic population of $\sim 10^5$ active radio pulsars. Radio pulsars are observed through their emission of broadband radio noise in the form of a periodic sequence of pulses. The periodicity indicates the rotational frequency. The fastest pulsar spins at a frequency of 716 Hz, while the slowest ones spin between 1 and 0.1 Hz. The pulse phenomenon is produced by a beamed cone that is observed when pointing towards the Earth like a beacon. The radio pulse generating mechanism is still not fully understood. Although it is known that the energy source is the angular momentum, converted through the strong dipolar magnetic field. This idea is founded in the observational fact that the pulsars slow down. When plotting the pulse period and its derivative in a $\mathrm{P}-\dot{\mathrm{P}}$ diagram, as in figure 2.1, the pulsars separate into two groups. A large population of slow pulsars that spin down rapidly (the timescale $\mathrm{P}/\dot{\mathrm{P}} \sim 10^6 - 10^7$ yr) and a smaller population of fast pulsars called *millisecond pulsars* that spin down more slowly (timescale $\mathrm{P}/\dot{\mathrm{P}} \sim 10^8 - 10^9$ yr). Assuming the magnetic dipole radiation is the main energy radiation source sets a limit on the magnetic field strengt $B \propto \left(\mathrm{P\dot{P}}\right)^{1/2}$. Slow radio pulsars have magnetic fields of the order of 10^8 T, while millisecond pulsars have fields of the order of 10^4 T. Most of the millisecond pulsars ($\geq 80\%$) are found in binaries, whereas only about 1% of slow pulsars are in binaries. In figure 2.1 one identifies a large grey unpopulated area for large periods and small period derivatives. It is thought that neutron stars inside this area, the *pulsar graveyard*, have their radio emission switched off. Neutron stars inside the graveyard will only emit thermal radiation from their cooling surfaces. All new born radio pulsars found in SNRs have short periods and fast spin down timescales, while no millisecond pulsar has been found near SNRs. This observation has led to the idea that young pulsars are born with periods between 10^{-2} s and 10 s, while the fast millisecond pulsars are old and have their short periods due to a different mechanism. This difference can be explained by analyzing the case of a binary of two main sequence stars where one of them fills out the criteria to form a neutron star. The most massive star will burn out faster than its companion, and will explode as a type II supernova, leaving a neutron star remnant. If the binary is not disrupted, accretion can start and the outer layers of the companion are ripped off by gravitational pull exerted by the neutron star, see appendix A. If enough mass is accreted, the added angular momentum will spin the neutron star up from periods of tens of seconds to milliseconds (further details in section 2.2). If the accretion stops the neutron star will become a regular radio pulsar. In figure 2.1 this transformation corresponds to moving the neutron star from the graveyard to the bottom left corner. This process is called the *recycling scenario*, where a dead radio pulsar is recycled into a millisecond radio pulsar. Indeed, all of the observed pulsars in this region are in a binary system. The magnetic field decays by four to five orders of magnitude during the spin up phase, a transformation which currently has no explanation. The accretion is a possible candidate.

2.2 Neutron stars in binaries

Some of the accreting neutron stars are born in binaries that survive the supernova explosion that created the neutron star. In dense stellar regions such as globular clusters some lonely neutron stars may be able to capture companions. In either case, mass may be transferred from the companion to the neutron star. As mass falls down angular momentum is transferred to the neutron star and gravitational energy is partially released in form of radiation. The energy released in accretion is enormous. If all the energy is radiated the expected accretion luminosity is : $L_{accretion} = GM_{NS}\dot{M}/R_{NS}$, where G is the gravitational constant, M the neutron star mass, $\dot{M}$ the accretion rate and R the neutron star radius. Inserting regular neutron star values gives an efficiency close to 10% of the rest mass energy. These radiations will be in the X-ray spectrum. If the magnetic field is strong enough, accreted matter will be guided along the field lines and fall onto the magnetic polar caps, as in figure 2.2. If the magnetic poles are inclined compared to the rotational poles the observed radiation will have a pulse form, with the same frequency as the rotation, and be shifted by the *Doppler effect*. The mass of the companion star will separate the accreting neutron stars in three different subtypes:

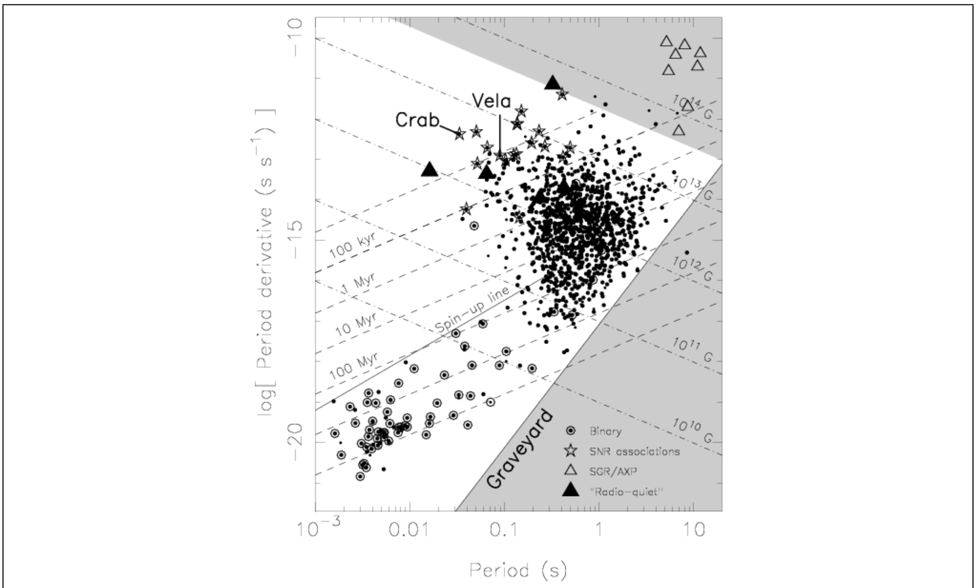

Figure 2.1: P-$\dot{\text{P}}$ diagram. The younger pulsars as the Crab and Vela indicate the start of the trajectory a neutron star will follow along its life: going to the lower right where a big population lies before fading out in the graveyard. The recycled ones in the millisecond section belong to binaries. The white triangles, the SGR, or magnetars are separated from the rest. The ages, magnetic field strenght, the spin and its spin down rate are read from the graph.

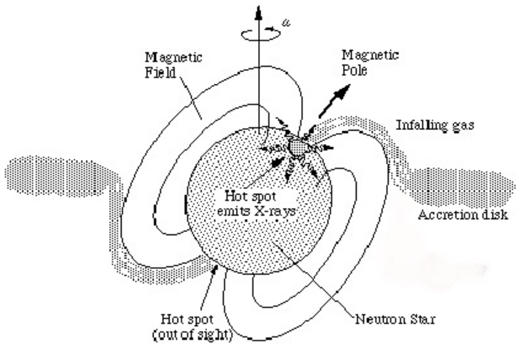

Figure 2.2: Accretion along field lines. Once the matter falls beneath the magnetospheric radius they follow the field lines onto the poles[13].

2.2.1 Low Mass X-Ray Binaries: LMXRB

If the companion star has less mass than the Sun, the mass transfer occurs via Roche lobe overflow, as explained in appendix A. If part of the companion star's envelope is close enough to the neutron star, the neutron star's gravitational attraction on that part of the envelope is greater than the companion star's attraction, with the result that the gas in the envelope falls onto the neutron star. However, since the neutron star is tiny, astronomically speaking, the gas has too much angular momentum to fall on the star directly and therefore orbits around the star creating an accretion disk[14]. Within the disk, magnetic or viscous forces operate to allow the gas in the disk to drift in slowly as it orbits, and to eventually reach the stellar surface. If the magnetic field at the neutron star's surface exceeds about 10^4 T, then the field can couple strongly to the matter before it reaches the surface. As matter and field couple the field lines guide the infalling matter onto the magnetic poles. The friction of the gas with itself as it spirals in towards the neutron star heats the gas to millions of degrees, and causes it to emit X-rays. Once on the surface of the star the accreted mass piles up on the magnetic poles until enough mass, and therefore pressure, is present to trigger a thermonuclear fusion of accreted light material into iron. This process is detailed in section 2.2.4.

2.2.2 Intermediate Mass X-Ray Binaries

If the companion has between one and ten solar masses the mass transfer is unstable and does not last long. The Roche lobe overflow will be very large and the companion star will quickly become a LMXRB. No IMXRB have been observed, which indicates that the IMXRB-stage is very short on astrophysical timescales.

2.2.3 High Mass X-Ray Binaries

If the companion has mass above 10 solar masses, mass transfer can occur through two different ways when the star has reached its supergiant stage. Both of the stars are visible in a HMXRB, the companion in optical wavelength and the neutron star in X-rays.

Supergiant Roche lobe Overflow X-Ray Binaries

When a massive star reaches the last stages of its life, after having consumed most of the hydrogen in its core, the outer layers begin to expand and the star grows enormously. It becomes a supergiant. As it grows the gravitational pull on its outer layers decreases. The supergiant can then expand out of the Roche lobe and start to feed the neutron star. However, the star does not need to expand out of the Roche lobe to feed the neutron star.

Supergiant Stellar Wind X-ray Binaries

High mass stars are very luminous, and matter in the atmosphere is continuously pushed out by the high energetic photon wind. They push a stream of particles along with them. These particles dissipate into the empty space around the star at very high velocities. This is called a radiation-driven stellar wind. The neutron star will then pick up some of the dissipated matter and start the accretion process, becoming a weak X-ray source.

Figure 2.3: An artist's impression of the High Mass X-ray Binary Cygnus X-1. The Roche lobe overflow is clearly visible as matter falls down. The compact object is a black hole, but the accreting process is identical as in the neutron star case[1].

2.2.4 Accreting millisecond X-ray pulsar

In between the young radio pulsars and the old millisecond pulsars one expects to have accreting millisecond X-ray pulsars. The accreting millisecond X-ray pulsars have strong enough fields to lead all the infalling matter onto the star's poles as in figure 2.2. As the matter falls onto the poles, two hotspots exist on the star surface. The pulsar emits X-ray pulsations due to the rotation, the same oscillation as in radio pulsars.

After the accretion phase, the companion is destroyed by the powerful radiation or winds, or leaves the pulsar or leaves a remnant (white or brown dwarf). Left is an isolated pulsar or a pulsar in a binary, a rotation powered millisecond pulsar. Accreting millisecond pulsars are therefore expected to be the link between the well observed young radio pulsars and the old millisecond pulsars. The first accreting millisecond pulsar was discovered in 1998. The light mass accreting X-ray binary SAX J1808.4-3658 was the proof of existence. However there are still unresolved questions: the theory predicts periods ranging from the seconds to sub-milliseconds, while the fastest observed spin at 1.4 ms, meaning there is a gap in the populated periods[5].

Accretion theory

The accretion disc is cut off by the neutron magnetic field lines at the magnetospheric radius $r_m \sim r_A$, where

$$r_A = \left(\frac{\mu^4}{2GM\dot{M}^2} \right)^{1/7},$$

is the *Alfven radius*, $\mu = \frac{B_0 R^3}{2}$ is the magnetic moment of the neutron star B field, and B_0 is the magnetic field at the poles. Defining the co-rotation radius:

$$r_{co} \equiv \left(\frac{GM}{\omega^2} \right)^{1/3},$$

which is the radius at which the Keplerian gas velocity equals the star's rotational velocity. If the co-rotating radius is larger than the magnetospheric radius the accreted matter will contribute with a positive torque on the neutron star, while if not it will absorb angular momentum and slow down the star's rotation.

Transfer of angular momentum

As matter falls down the total angular momentum is conserved. Given by

$$\vec{L} = \int \vec{r} \times \mathrm{d}\vec{p},$$

As matter falls down on the star with higher angular velocity, the total angular momentum is conserved through an increase in the star's angular momentum. If the star spins fast enough the centrifugal effect will deform the star into a momentum quadrupole, which in turn will radiate *gravitational waves* and hence dissipate energy. The star will increase its rotational velocity as long as the incoming rotational energy surpasses the energy radiated through gravitational waves and electromagnetic radiation.

X-ray burst

The accretion process is much more efficient than nuclear fusion, in terms of energy released: Hydrogen fusion liberates 5 MeV per fused atom, while accretion liberates 200 MeV per nucleus. The emitted radiation is black body radiation with peak in the soft X-rays and therefore the fusion process is unobservable in the shadow of the accretion radiation. However, if the nuclear radiation occurs over a smaller timescale than the accretion it can dominate the radiation. Indeed, observed in many LMXBs are the *Type I X-ray bursts*[14], a sudden release of nuclear energy, observed in the X-rays, with a sudden rise of the order of seconds with exponential decay lasting of the order $10-10^3$ s, corresponding to the cooling of the burnt layer. The matter burnt can be composed in three different ways:

- a mix of hydrogen and helium,
- pure helium,
- carbon,

where the released energy and duration of carbon fusion is two to three orders of magnitude larger than for the other possibilities. The carbon fusion burst is known as *superburst*. In 2007 a detected burst lasted 20 minutes and radiated $6.5 \cdot 10^{32}$ J, and the radiating zone was no larger than a golf field.

A second type of burst exists: Believed to occur when a sudden increase of accretion takes place. The increase in accretion means an equal increase in radiations. The burst often decays equally fast. It is noteworthy, these burst have only been observed in two sources. This type of burst is called *Type II X-ray bursts*.

2.2.5 Magnetic field

Neutron stars possess an extremely strong magnetic field. But where do these magnetic fields come from? The traditional assumption is that they are inherited from the progenitor star. All stars have weak magnetic fields, and those fields can be amplified simply by the act of compression. According to Maxwell's equations of electromagnetism, as a magnetized object shrinks, the field strengthens quadratically. If the core magnetic field started with sufficient strength, this compression could explain pulsar magnetism. Unfortunately, the magnetic field deep inside a star cannot be measured, so this simple hypothesis cannot be tested. But it would seem it is only a part of the solution: Within a star, gas can circulate by convection. Warm parcels of ionized gas rise, and cold ones sink. Because ionized gas conducts electricity well, any magnetic field lines threading the gas are dragged with it as it moves. The field can thus be changed and sometimes amplified. This phenomenon, known as *dynamo action*, is thought to be the main process behind the magnetic field of stars and planets. But for the dynamo action to operate the turbulent core has to rotate rapidly enough. A brief period after the birth of a neutron star the convection is especially violent. Computer simulations[11] found that temperatures in a newborn star exceeds 30 billion kelvins. Hot nuclear fluid convexes with period 10 milliseconds or less, carrying enormous kinetic energy. After about 10 seconds, the convection ceases. For the dynamo to operate globally (rather than in limited regions) the star's rate of rotation has to be comparable to its rate of convection. Deep inside the sun, these two rates are similar, and the magnetic field is able to organize itself on large scales. In the sun the convection gives about 10% of its kinetic energy to the magnetic field. By analogy, a neutron star born rotating as fast as, or faster, than the convective period of 10 milliseconds could develop a widespread, extremely strong magnetic field. These hypothetical neutron stars have been named *magnetars*. However an upper limit to neutron star magnetism exists, and is of the order of 10^{11}Tesla. Beyond this limit, the fluid inside the star will mix and the field dissipate. No known objects in the universe can generate and maintain fields stronger than this level. As a consequence of these results radio pulsars, with fields much weaker than the one found, are neutron stars in which the large-scale dynamo action has **failed** to operate. As example the newborn Crab pulsar rotated once every 20 milliseconds, much slower than the rate of convection, so the dynamo action never acted.

2.3 Magnetars

A *magnetar* is a neutron star characterized by an extremely powerful magnetic field. This field powers emission of high-energy electromagnetic radiation. Magnetars are *soft gamma repeaters*, objects which emit large bursts of gamma-rays and X-rays at irregular intervals. A powerful gamma-ray burst was detected on March 5, 1979 by different detectors in our solar system (Soviet and American probes and on Earth), and the origin was triangulated to a near supernova remnant in the Large Magellanic Cloud. It soon became clear that this burst was not a normal GRB[1]; the photons were less energetic, and several bursts followed later from the same origin. According to the theory where magnetars are the origin of these gamma-rays the burst would cause the object to slow down its rotation. And indeed they do. Having a period of order seconds to tens of seconds they spin much slower than ordinary neutron stars. Observation over five years of SGR 1806-20 showed oscillations with a period of 7.47 seconds increase by two parts in 1,000. Such an increase implies a magnetic field approaching 10^{11}Tesla. As late 2012, 21 magnetars are known, with several new candidates. Figure 2.1 clearly shows the magnetars as neutron stars with high spindown rate and low frequency. For more information about the neutron stars, see the article which was used as guide[14].

[1] A GRB is a flash of gamma rays, the brightest in the universe, lasting from milliseconds to several minutes. GRBs are thought to come from the collapse phase of a supernova, or when compact objects in binaries merge.

Chapter 3

Physics of neutron stars

3.1 Gravitation

Being so dense neutron stars exhibit enormous gravitational forces, only exceeded by black holes. The gravitational forces at the surface of a neutron star with the standard radius and mass, $R = 10^4$ m and $m = 1.44\ M_\odot$, on an object with mass m is

$$\begin{aligned} F &= G\frac{mM}{R^2} \\ &= 6.67 \cdot 10^{-11}\frac{m \cdot 1.44 \cdot 1.98 \cdot 10^{30}}{(10^4)^2} \\ &= 1.98 \cdot 10^{12} \cdot m \text{ N}, \end{aligned}$$

which is equivalent to $2 \cdot 10^{11}$ times stronger than the gravity at the surface of Earth.

To show the extreme force a simple example is taken: a (heavy) mug of coffee of 1.0 kg falling from 1.0 m. A casual situation on Earth. The relativstic energy is given by

$$E = mc^2 \cdot \frac{\sqrt{1 - \frac{2GM}{Rc^2}}}{\sqrt{1 - \frac{v^2}{c^2}}}.$$

Where the nominator is due to general relativistic corrections and the denominator, also written as $1/\gamma$, to special relativistic corrections. Using energy conservation the speed can be found:

$$E = mc^2 \cdot \sqrt{1 - \frac{2GM}{R_1c^2}} = mc^2 \cdot \frac{\sqrt{1 - \frac{2GM}{R_2c^2}}}{\sqrt{1 - \frac{v_2^2}{c^2}}},$$

$$1 - \frac{2GM}{R_1c^2} = \frac{1 - \frac{2GM}{R_2c^2}}{1 - \frac{v_2^2}{c^2}},$$

$$1 - \frac{v^2}{c^2} = \frac{1 - \frac{2GM}{R_2 c^2}}{1 - \frac{2GM}{R_1 c^2}}.$$

Rearranging and omitting some details yields

$$\begin{aligned} v &= c\sqrt{1 - \frac{1 - \frac{2GM}{R_2 c^2}}{1 - \frac{2GM}{R_1 c^2}}} \\ &= 0.0086c \\ &= 2.6 \cdot 10^6 m/s. \end{aligned}$$

These simple calculations make it clear that the gravitational forces on the neutron star are extreme. However, on charged particles it is a different story, as will be seen in section 4.

Not only are the forces extreme, but other effects, like lightbending becomes important. Even though its relevance for the paper is minimal the next section takes a closer look on lightbending, for the curiosity and fun.

3.1.1 Light bending in Schwarzschild geometry

The *Schwarzschild metric* dictates light bending around compact objects. In contrast to Newtonian Geometry, light is affected by mass. In General Relativity it is "just another" test particle, on equal footing as the rest of them. The start point is the *Lagrangian* which is equal to 0 since the photon is massless, written in the ρ coordinate, in the $\theta = \frac{\pi}{2}$ plane, with J_z as the canonical momentum associated with ϕ, and $-E$ as the canonical momentum for t.

$$0 = L = \frac{1}{2}\left(J_z^2 \rho^2 - \frac{E^2 \rho^4 - \dot{\rho}^2}{\rho^4 (1 - 2M\rho)}\right).$$

Rearranging yields:

$$\frac{\dot{\rho}^2}{J_z^2} = \rho^4 \left(\frac{E^2}{J_z^2} - \rho^2 + 2M\rho^3\right).$$

Switching to ϕ derivatives through $\dot{\rho} = \rho' J_z \rho^2$ and employing the Lagrange equations one gets:

$$\rho'' = -\rho + 3M\rho^2.$$

The linear term in M is the difference between general relativity and Newtonian mechanics. Employing perturbation and substituting again to $\rho = \frac{\sin\phi}{R} + \epsilon\tilde{\rho}$ yields:

$$-\frac{1}{R}\sin\phi + \epsilon\tilde{\rho}'' = -\left(\frac{1}{R}\sin\phi + \epsilon\tilde{\rho}\right) + 3M\left(\frac{1}{R}\sin\phi + \epsilon\tilde{\rho}\right)^2$$

Associating the expansion parameter ϵ with the mass M of the gravity-producing object yields the equation for $\tilde{\rho}$ to first order in $\epsilon \sim M$:

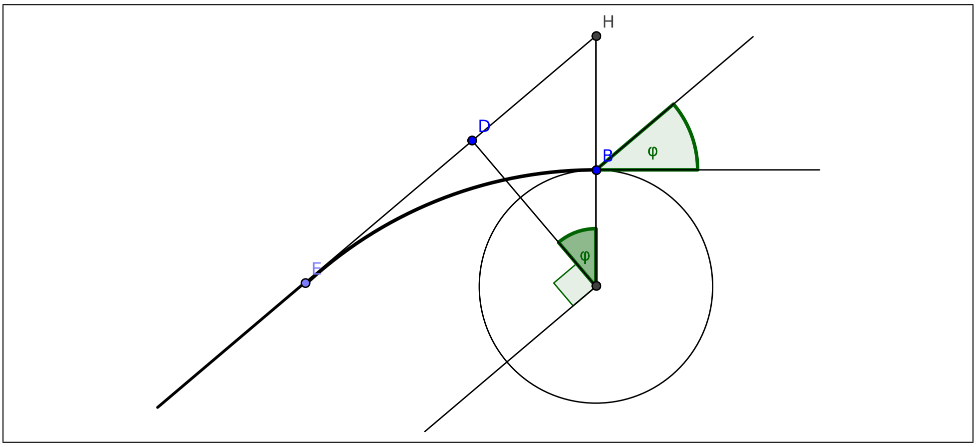

Figure 3.1: Lightbending near the neutron star. The thick line is the light trajectory, clearly deviated by the neutron star's gravitational field. The image shows how normally hidden parts in flat space-time are visible due to lightbending.

$$\tilde{\rho}'' = -\tilde{\rho} + \frac{3}{R^2}\sin^2\phi,$$

with solution:

$$\rho(\phi) = \frac{\sin\phi}{R} + M\frac{(1+\cos^2\phi)}{R^2}.$$

Using as initial value at infinite distance to the compact object $\rho = 0$:

$$\begin{aligned} 0 = \rho(\phi) &\simeq \frac{2M}{R^2} + \frac{\phi}{R}, \\ \Rightarrow \phi &= -\frac{2M}{R}. \end{aligned} \tag{3.1}$$

Assuming that all emitted photons are emitted from the surface with an isotropic distribution one can calculate how much of the star's surface is visible to an observer infinitely far away.

In the classical Newtonian case, half of the star would be visible, corresponding to π radians of the cross section. With light bending however, more will be visible and the star will seem bigger, as illustrated by figure 3.1. Outgoing photons from point B on the surface with tangential direction will be bent by the gravitational field of the star to arrive at point E where the gravitational field practically does not affect any more, making it visible to the observer. To the observer these photons will seem to come from point H, and therefore indicate that the radius ends at point D.

The R used in the formulas above corresponds to the distance between the straight line and the center of the star, that is, the distance from the center to the point D in the figure, which corresponds to the apparent radius to the observer. The closest point along the photon trajectory is defined by :

$$r_{min} = \frac{R^2}{M+R} = r_{NS}.$$

Using as radius $r_{NS} = 10^4$m one can find R:

$$R^2 - r_{NS}R - Mr_{NS} = 0,$$

$$\Rightarrow R = \frac{r_{NS} \pm \sqrt{r_{NS}^2 + 4Mr_{NS}}}{2}.$$

Only the $+$ sign gives physical meaning, thus $R = 1.186 \cdot 10^3$m. Employing equation 3.1 yields

$$\phi = 2\,\frac{2.21 \cdot 10^3}{1.186 \cdot 10^4} = 0.37. \tag{3.2}$$

The observer will observe a portion p of the surface of the star:

$$\begin{aligned}
4\pi R^2 - \int_0^{\psi} 2\pi R^2 \sin\theta \mathrm{d}\theta &= 4\pi R^2 - 2\pi R^2 \left(1 - \cos\psi\right) \\
&= 2\pi R^2 \left(1 + \cos\psi\right) \\
\text{where } \psi = \pi/2 - \phi & \\
&= 2\pi R^2 \left(1 + \sin\phi\right).
\end{aligned}$$

Written in term of proportion of the whole surface:

$$p = \frac{1 + \sin\phi}{2}. \tag{3.3}$$

To find the proportion, the neutron star mass M has to be expressed in meters, such that ϕ is dimensionless:

$$\begin{aligned}
M &= m_{NS} \cdot G \cdot c^{-2} \\
&= 1.44 \cdot 1.989 \cdot 10^{30} \cdot 6.67 \cdot 10^{-11} \cdot \frac{1}{\left(3.00 \cdot 10^8\right)^2} \\
&= 2.21 \cdot 10^3\text{m},
\end{aligned}$$

which in turn, combining the result 3.3 and 4.7 yields

$$\boxed{p = 0.68}$$

An increase of apparent radius of 1.186 means an increase of apparent volume of $1.186^3 = 1.668$. This effect is visible in figure 3.2, where a large percentage of the surface is visible. Without the lightbending the poles would be at the extremity of the visible surface, but with lightbending the poles are clearly visible and a substantial area beyond the poles is visible.

For further details, read the lecture notes used as inspiration[4].

Another interesting effect is the emission of gravitational waves. A shallow description of the effect follows in the next section.

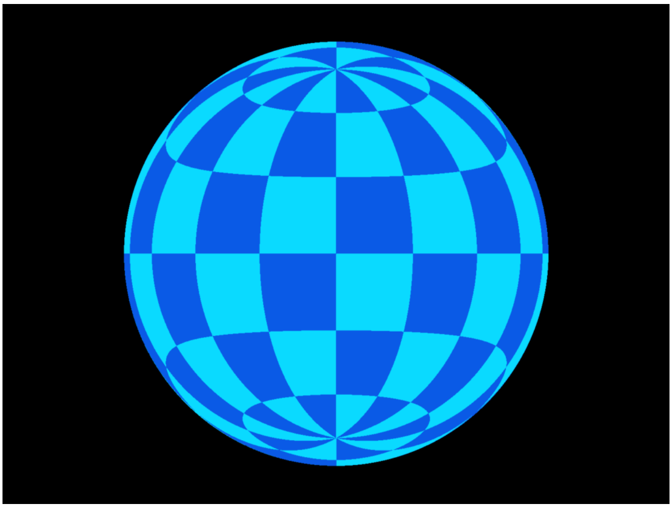

Figure 3.2: The visible star surface. In flat space-time only 6×6 cells would be visible, whereas here two cells extra are visible at the horizon. Image taken from spacetimetravel.org[2].

3.1.2 Gravitational waves

According to GR and SR, gravity is mediated with the speed of light. As the source of gravity changes in space a wave appears due to the difference in amplitude. In the case of a rotating source this wave is sinusoidal. Looking at neutron stars the mass distribution and shape is relevant. If the star is spherical, the gravitational attraction on an object is independent of the rotational phase of the star, hence no gravitational wave is emitted. On the other hand, if the star has an inertial quadrupole moment the amplitude of the attraction is dependent of the phase. The simplified case of a binary system with identical point masses shows the concept:

$$F \propto \frac{1}{R_1^2} + \frac{1}{R_2^2}.$$

Finding the attraction on an observer a distance α from the center of mass in two different cases: when the point masses and observer are aligned: $R_1 = \alpha + \beta$, $R_2 = \alpha - \beta$, and a quarter of cycle later: $R_1 = R_2 = \sqrt{\alpha^2 + \beta^2}$. The point masses are circulating at a distance β around the center of mass.

$$\begin{aligned} F_1 &\propto \frac{1}{(\alpha+\beta)^2} + \frac{1}{(\alpha-\beta)^2} \\ &\propto \frac{(\alpha+\beta)^2 + (\alpha-\beta)^2}{(\alpha+\beta)^2(\alpha-\beta)^2} \\ &\propto 2\frac{\alpha^2+\beta^2}{(\alpha+\beta)^2(\alpha-\beta)^2}, \end{aligned}$$

while

$$F_2 \propto \frac{2}{\alpha^2 + \beta^2}.$$

Inserting some test values $\alpha = 2$ and $\beta = 1$ yields $F_1 = \frac{10}{9}$ and $F_2 = \frac{2}{5}$ which clearly are not the same. This simple case shows that the attraction is not time independent. These waves carry energy, hence energy is lost from the rotating system. The energy radiated depends on the rotation frequency and the quadrupole moment. In the neutron star case the shape is very close to spherical so the radiated energy is negligible, unless the star spins very rapidly, which in turn can lead to deformations, or mountains confined by the electromagnetic field appears.

3.2 Maxwell's equations

The electromagnetic force is one of the four fundamental forces. It is described by the electromagnetic fields and acts on magnetic or electric charged poles (monopole or higher order poles). Classical electromagnetism is a classical approximation of *quantum electrodynamics* valid in microscopic and higher scales, and can be described by *Maxwell's equations*, a set of partial differential equations (or by an equavilent set of integral equations):

Maxwell's equations in differential form:

$$\nabla \cdot \vec{\mathcal{E}} = \frac{\rho}{\epsilon_0} \text{ which is called } \textit{Gauss' law}, \tag{3.4a}$$

$$\nabla \cdot \vec{B} = 0, \tag{3.4b}$$

$$\nabla \times \vec{\mathcal{E}} = -\frac{\partial \vec{B}}{\partial t}, \tag{3.4c}$$

$$\nabla \times \vec{B} = \mu_0 \vec{J} + \mu_0 \epsilon_0 \frac{\partial \vec{\mathcal{E}}}{\partial t}. \tag{3.4d}$$

3.2.1 Gauss' law

Neutron stars are superconductors, and therefore there can be no electric field inside the star. Hence the electric field must be canceled out by surface charges. Writing Gauss's law in integral form one gets:

$$\frac{Q}{\epsilon_0} = \oint_S \vec{\mathcal{E}} \cdot \mathrm{d}\vec{A}, \tag{3.5}$$

Employing what is called a *Gauss pillbox* around the surface of the star where all walls are either normal or parallel to the surface one can easily calculate the surface charge. Placing the box where the field is entirely normal one gets:

$$\frac{\sigma A}{\epsilon_0} = \vec{\mathcal{E}} \cdot \vec{A},$$

$$\sigma = \epsilon_0 \mathcal{E}_{normal}. \tag{3.6}$$

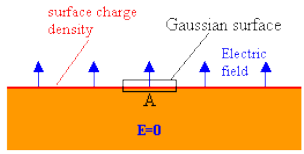

Figure 3.3: Gauss pillbox around the surface of the star, with sides either normal or parallel to the surface. Image taken from lecture notes[17].

3.3 Dipole radiation

The magnetic field in a neutron star is simplified to a magnetic dipole. Employing this, whilst observing the period and spin down torque, the magnetic field strength is not far away. Dipole radiation states[6]:

$$I\dot{\omega} = -\frac{2}{3c^3}B^2R^6\omega^3\sin^2\alpha, \tag{3.7}$$

Where I is the moment of inertia, ω its spin frequency, B the polar field strength at the surface, R the star's radius and α the angle between the magnetic axis and the spin axis of the star. Since there currently is no clear theoretical prediction of the dependence of the spin down torque on α for a real neutron star with plasma filled magnetosphere (while 3.7 is only valid in vacuum) the α-dependence is omitted. This simplification is justifiable since $\sin^2\alpha \in [0, 1]$. Rearranging the equation one gets

$$B = \left(\frac{3c^3IP\dot{P}}{8\pi^2R^6}\right)^{1/2} = 3.2\times10^{15}\left(P\dot{P}\right)^{1/2}\ \mathrm{T},$$

where P is the period and $\dot{P}$ is the spin down rate. Inserting the period of 0.0331 s and its derivative $4.22\cdot10^{-13}$ s/s yields a field of $B = 3.78\cdot10^8$T.

3.4 The Lorentz force

3.4.1 Change of frame

In the inertial frame of reference observed from Earth the forces acting on a charged particle at the surface of the star are both electric and magnetic. The rotating reference frame is not an inertial frame, hence a Lorentz transformation cannot transform between the two frames. Fictitious forces appear in the rotating frame: the *centrifugal force* and if the object of interest is in motion in the rotating frame the *Coriolis force*. Considering the fictitious forces as real forces in the rotating system it can be considered as an inertial frame.

$$\vec{F}_{Lorentz,1} + \vec{F}_g = \vec{F}_{Lorentz,2} + \vec{F}_g + \vec{F}_{Coriolis} + \vec{F}_{centrifugal}$$

where the Lorentz force is given by:

$$\vec{F}_{Lorentz} = q\left(\vec{\mathcal{E}} + \vec{v} \times \vec{B}\right)$$

The gravitational force is identical in both frames, the Coriolis force only acts on particles in motion in the rotating frame, so for a particle at rest on the surface its contribution is zero. In the case where the centrifugal fictitious force is negligible one gets:

$$\vec{F}_{Lorentz,1} = \vec{F}_{Lorentz,2} + \vec{F}_{centrifugal} \simeq \vec{F}_{Lorentz,2}$$

$$q\left(\vec{\mathcal{E}}_1 + \vec{v}_1 \times \vec{B}_1\right) = q\left(\vec{\mathcal{E}}_2 + \vec{v}_2 \times \vec{B}_2\right)$$

where the subscript index 1 refers to the one observed from Earth and the index 2 refers to the one corotating. In the corotating one the velocity is $v = 0$.

$$\vec{\mathcal{E}}_2 = \vec{\mathcal{E}}_1 + \vec{v}_1 \times \vec{B}_1 = \frac{1}{q}\vec{F}_{Lorentz} \tag{3.8}$$

3.5 Magnetic flux

A good approximation in the case where the dynamo action fails is to only rely on the conservation of magnetic flux through the equatorial plane inside the star throughout the collapse. The flux is defined as the surface integral

$$\Phi = \int_S \vec{B} \cdot d\vec{A},$$

where $\vec{B}$ is the magnetic field vector. The total flux out of a closed surface is zero since no magnetic monopole exists. Ignoring the geometry of the magnetic field one will get the relation between the field strength and the radius:

$$B_i \pi R_i^2 = B_f \pi R_f^2.$$

To find the value of the magnetic field strength of a neutron star one needs the one of the original core. Using the strongest field strength observed in a white dwarf with value $B \approx 5 \times 10^4$ T as an extreme case scenario, which is a lot stronger than a typical white dwarf magnetic field of 10 T. Using the extreme case yields:

$$B_{NS} \approx B_{WD}\left(\frac{R_{WD}}{R_{NS}}\right)^2 = 1.3 \times 10^{10}\ \mathrm{T}.$$

The field is of the same order of magnitude as when calculated taking into account convections[6]. One might guess that the white dwarf also has let the dynamo action build up the field. This field corresponds to the one from a magnetar.

3.6 The Equation of State

3.6.1 The Fermi pressure

All fermions, particles with half integer spin, obey the *Pauli exclusion principle*. This principle only allows one fermion per quantum state. When many non-thermal fermions are together they fill up the lower energy orbitals. Taking electrons as examples: the two first electrons, two since there are two different possible spins, up and down, occupy the lowest energy states nearest the nucleus. As more and more electrons are added they fill up the higher energy states. These higher energy shells support the electrons against the attractive electric forces of the nucleus. This phenomena gives rise to the *Fermi degeneracy pressure* when matter gets squeezed together and electrons are prohibited to take the same quantum states: As matter gets compressed, the uncertainty in position Δx becomes smaller. Then, as dictated by the *Heisenberg's uncertainty principle*, $\Delta x \Delta p \geq \frac{\hbar}{2}$, the electron momenta uncertainty Δp becomes larger. Thus, even at zero temperature, the electrons travel at a minimum speed which gives rise to the pressure. When this pressure exceeds the thermal pressure the electrons are referred to as *degenerate*. In a white dwarf the gravitational force is kept at bay by the electron degeneracy pressure. However, in a neutron star, where this pressure did not suffice, the pressure preventing collapse is the neutron degeneracy pressure.

Since neutrons exclude each other, a volume with characteristic size $\lambda \sim \frac{R}{N^{1/3}}$ can be awarded to each one of them, where N is the total number of neutrons and R the neutron star radius. The *Fermi momentum*, defined as the momentum of the highest filled quantum state at zero temperature, is given as

$$p_F \sim \frac{\hbar}{\lambda} \sim N^{1/3}\frac{\hbar}{R}. \tag{3.9}$$

As the sphere is compressed, the radius R shrinks hence p_F rises and work has to be done to compress. Using a relativistic approximation the energy is

$$E = \sqrt{p_F^2 c^2 + m^2 c^4} \simeq p_F c,$$

yielding a total energy

$$E_F \simeq N p_F c \simeq N^{4/3}\frac{\hbar c}{R}.$$

In a neutron rich system these supply the most gravitational energy E_G:

$$E_G \sim -G\frac{(m_n N)^2}{R}.$$

For large N the total energy will become negative and the energetically favorable state is collapse. The critically particle number N is given by

$$N_{crit} \simeq \left(\frac{\hbar c}{G m_n^2}\right)^{3/2} \simeq 2.2 \times 10^{57}. \tag{3.10}$$

Assuming relativistic neutrons $E_F = p_F c \geq mc^2$, using equations 3.9 and 3.10 gives the radius

$$R \leq \frac{\hbar}{mc}\left(\frac{\hbar c}{G m_n^2}\right)^{1/2} \simeq 2.75 \times 10^3 \text{ m}.$$

Of course this is a very crude model. A more accurate model, but still simplified, is the one of the star as a degenerate gas.

3.6.2 Degenerate gas

The exact EoS in a neutron star is unknown. However, since the EoS is of such importance the ideal fermion gas is chosen obeying the *Fermi-Dirac statistics* at zero temperature. The distribution function is as follows:

$$f(E) = \frac{1}{e^{(E-\mu)/kT} + 1}. \tag{3.11}$$

For completely degenerate fermions μ becomes the Fermi energy E_F and

$$f(E) = \begin{cases} 1 & \text{if } E \leq E_F \\ 0 & \text{if } E > E_F \end{cases}$$

Which is a valid approximation for a cold gas, where the Fermi energy is much larger than the thermal one:

$$\left(p_F^2 c^2 + m_n^2 c^4\right)^{1/2} - m_n c^2 \gg kT.$$

The number density of neutrons is given by:

$$n_n = \frac{2}{\hbar^3}\int_0^{p_F} 4\pi p^2 \mathrm{d}p = \frac{8\pi}{3\hbar^3} p_F^3 = \frac{1}{3\pi^2 \lambda_n} x^3,$$

where $x = \frac{p_F}{m_n c}$ is the dimensionless *Fermi momentum* and $\lambda_n = \frac{\hbar}{m_n c}$ is the *neutron Compton wavelength*. The index F is omitted from now on. The pressure per particle is $P = \frac{nk^2}{3\epsilon}$, where ϵ is the energy, hence the total pressure is given by:

$$P_n = \frac{1}{3}\frac{2}{\hbar^3}\int_0^{p_F} \frac{p^2 c^2}{(p^2 c^2 + m_n^2 c^4)^{1/2}} 4\pi p^2 \mathrm{d}p = \frac{m_n c^2}{\lambda_n^3}\phi(x). \tag{3.12}$$

where ϕ is a function of the variable x as follows:

$$\phi(x) = \frac{1}{8\pi^2}\left[x\left(1+x^2\right)^{1/2}\left(\frac{2x^2}{3} - 1\right) + \ln\left[x + (1+x^2)^{1/2}\right]\right] \to \begin{cases} \frac{x^5}{15\pi^2} & x \ll 1 \\ \frac{x^4}{12\pi^2} & x \gg 1 \end{cases}$$

To first order the mass is due to the neutrons:

$$\begin{aligned} \rho &\simeq m_n n_n \\ &= \frac{m_n}{\lambda_n^3}\frac{1}{3\pi^2} x_n^3 \\ &= 6.107 \times 10^{18} x_n^3 \text{kg m}^{-3}. \end{aligned} \tag{3.13}$$

The mass density is a function of the distance to the center and the mass $\mathrm{d}m$ inside a spherical shell with radius r and thickness $\mathrm{d}r$ is $\mathrm{d}m = 4\pi\rho(r)\mathrm{d}r$, hence

$$\frac{\mathrm{d}m}{\mathrm{d}r} = 4\pi\rho(r)r^2, \tag{3.14}$$

integrating the equation above:

$$m(r) = 4\pi \int_0^r \mathrm{d}r'\rho(r')r'^2.$$

The gravitational pull exerted on a part of the shell with area $\mathrm{d}A$ from the mass $m(r)$ inside the shell is given by Newton's law of gravity:

$$\begin{aligned}\mathrm{d}F &= -\frac{Gm(r)\mathrm{d}m}{r^2} \\ &= -\frac{Gm(r)\rho(r)\mathrm{d}r\mathrm{d}A}{r^2}.\end{aligned} \tag{3.15}$$

The opposing force is due to the pressure:

$$\begin{aligned}\mathrm{d}F &= \mathrm{d}A\,[P(r+\mathrm{d}r) - P(r)] \\ &= \mathrm{d}A\mathrm{d}P.\end{aligned} \tag{3.16}$$

The star is in hydrostatic equilibrium, meaning that the total force vanishes. Combining equations 3.15 and 3.16 yields

$$\frac{\mathrm{d}P}{\mathrm{d}r} = -\frac{Gm(r)\rho(r)}{r^2}. \tag{3.17}$$

Which takes into account the force of gravity. However, this simplification does not take account of relativity. And the neutron star is highly relativistic. Taking into account relativity, three new terms appear, transforming the equation above into what is called the *Tolman-Oppenheimer-Volkov equation*, the correct equation for hydrostatic equilibrium. The TOV equation is as follows

$$\frac{\mathrm{d}P}{\mathrm{d}r} = -\frac{G\epsilon(r)m(r)}{r^2}\left[1+\frac{p(r)}{\epsilon(r)}\right]\left[1+\frac{4\pi r^3 p(r)}{M(r)}\right]\left[1-\frac{2GM(r)}{r}\right]^{-1}. \tag{3.18}$$

However, since the TOV does not have an analytic solution, the equation 3.17, which is not relativistic, will be used instead. Since this explanation is only qualitative it is a justifiable choice. Using equation 3.14 yields:

$$\begin{aligned}\frac{1}{r^2}\frac{\mathrm{d}}{\mathrm{d}r}\left(\frac{r^2}{\rho}\frac{\mathrm{d}P}{\mathrm{d}r}\right) &= -\frac{G}{r^2}\frac{\mathrm{d}m}{\mathrm{d}r} \\ &= -4\pi G\rho(r).\end{aligned} \tag{3.19}$$

The ideal degenerate gas has an EoS of the form $P = P(\rho)$, where ρ can be expanded: $\rho = \rho_0 + \epsilon_n/c^2$. Employing this while combining equations 3.12 and 3.13 yields an EoS in a Newtonian *polytropic* form:

$$P = K\rho_0^\Gamma, \tag{3.20}$$

where K and Γ are constants, two limiting cases appear:

- Non-relativistic neutrons, $\rho \ll 6 \times 10^{18}$kg m^{-3}, $x \ll 1$

$$\Gamma = \frac{5}{3}, \quad K = \frac{3^{2/3}\pi^{4/3}}{5}\frac{\hbar^2}{m_n^{8/3}} = 2.134 \times 10^5.$$

- Extremely relativistic neutrons $\rho \gg 6 \times 10^{18}$kg m^{-3}, $x \gg 1$

$$\Gamma = \frac{4}{3}, \quad K = \frac{3^{1/3}\pi^{2/3}}{4}\frac{\hbar c}{m_n^{4/3}} = 7.747 \times 10^{10}.$$

For practical purpose Γ will be expressed as: $\Gamma = 1 + \frac{1}{n}$, where the n is known as the polytropic index. Expanding equation 3.19 using equation 3.20 yields

$$\frac{K(1+1/n)}{r^2}\frac{\mathrm{d}}{\mathrm{d}r}\left(r^2\rho^{1/n-1}\frac{\mathrm{d}\rho}{\mathrm{d}r}\right) = -4\pi G\rho(r). \tag{3.21}$$

At the radius R of the star the pressure is zero: $P(R) = 0$, hence the mass density vanishes too. The next step is to introduce the dimensionless variables θ and ξ defines as:

$$\theta^n = \frac{\rho}{\rho_c}, \tag{3.22}$$

$$\xi = \frac{r}{a}, \tag{3.23}$$

where ρ_c is the density at the center of the star $\rho_c = \rho(r = 0)$ and

$$a = \left[\frac{(n+1)K\rho_c^{1/n-1}}{4\pi G}\right]^{1/2}.$$

The new variables simplify equation 3.21 into the more elegant form

$$\boxed{\frac{1}{\xi^2}\frac{\mathrm{d}}{\mathrm{d}\xi}\xi^2\frac{\mathrm{d}\theta}{\mathrm{d}\xi} = -\theta^n.} \tag{3.24}$$

Equation 3.24 is known as the *Lane-Emden equation* for a star of polytropic index n.

The inner boundary condition corresponds to the center of the star, where the mass density is $\rho(0) = \rho_c$, hence $\theta = 1$. The second boundary condition requires some light manipulations: in the innermost layers of the star the mass inside the variable radius r is

$m(r) \sim 4/3\pi\rho_c r^3$. Combined with equation 3.17 yields $\frac{\mathrm{d}P}{\mathrm{d}r} \propto r$. Hence $\frac{\mathrm{d}P}{\mathrm{d}r} = \frac{\mathrm{d}\rho}{\mathrm{d}r} = 0$ for $r = 0$, which in turn means that the second boundary condition $\theta'(0) = 0$.

Equation 3.24 is in general analytically unsolvable and computer calculations are necessary. The star radius is given by

$$R = \left[\frac{(n+1)K\rho_c^{1/n-1}}{4\pi G}\right]^{1/2} \xi_1, \tag{3.25}$$

and the mass is given by

$$\begin{aligned} M &= 4\pi \int_0^R r^2 \rho \mathrm{d}r \\ &= 4\pi a^3 \rho_c \int_0^{\xi_1} \xi^2 \theta^n \mathrm{d}\xi \\ &= -4\pi a^3 \rho_c \int_0^{\xi_1} \frac{\mathrm{d}}{\mathrm{d}\xi}\left(\xi^2 \frac{\mathrm{d}\theta}{\mathrm{d}\xi}\right) \mathrm{d}\xi, \end{aligned} \tag{3.26}$$

where the limit ξ_1 corresponds to the radius of the star. Solving equation 3.25 with respect to ρ_c and inserting the found value in equation 3.26 yields the mass-radius relation for polytropes

$$M = 4\pi R^{(3-n)/(1-n)} \left[\frac{(n+1)K}{4\pi G}\right]^{n/(n-1)} \xi_1^{(3-n)/(1-n)} \xi_1^2 \|\theta'(\xi_1)\|. \tag{3.27}$$

Numerically one finds in the non-relativistic case $\xi_1 = 3.65375$ and $\xi_1^2\|\theta'(\xi_1)\| = 2.71406$ whereas in the ultrarelativistic case $\xi_1 = 6.89685$ and $\xi_1^2\|\theta'(\xi_1)\| = 2.01824$. In the ultrarelativistic case ($n = 3$) the mass is independent of the radius. However, in the neutron star case the neutrons are non-relativistic, letting the relativistic case irrelevant and more of a fun fact. In the non-relativistic ($n = 3/2$) case the relation takes the form $M \propto R^{-3}$. In the case of non-relativistic neutron stars the radius and mass are found to be:

$$R = 14.64 \left(\frac{\rho_c}{10^{18}\text{kg/m}^3}\right)^{-1/6} \text{km}, \tag{3.28}$$

$$M = 1.102 \left(\frac{\rho_c}{10^{18}\text{kg/m}^3}\right)^{1/2} \mathrm{M}_\odot, \tag{3.29}$$

where ρ_c is the unknown variable.

Remarks

This simple model is of course very crude, as the nucleons interact stronger than an ideal gas, where the strong forces are neglected.

Chapter 4

Calculations

The magnetic field of a neutron star is simulated as a superposition of two oscillating magnetic dipoles with a relative phase shift of a quarter of a cycle. Starting out with the field for a single dipole $\vec{m}_0 = m_0 \hat{z}$[10], using the substitution $t' = t - \frac{r}{c}$. The magnetic dipole moment is given by $\vec{m} = \vec{m}_0 \cos(\omega t)$.

$$\vec{A}(r,\theta,t) = \frac{\mu_0 m_0}{4\pi} \frac{\sin\theta}{r} \left[\frac{1}{r} \cos(\omega t') - \frac{\omega}{c} \sin(\omega t') \right] \hat{\phi}.$$

The electric and magnetic fields are found via the A-field:

$$\vec{\mathcal{E}} = -\frac{\partial A}{\partial t},$$

and

$$\vec{B} = \nabla \times A.$$

The curl will be separated into three different components:

$$\begin{aligned}
\left(\nabla \times \vec{A}\right)_r &= \frac{1}{r\sin\theta} \left(\partial_\theta (\sin\theta\, A_\phi) - \partial_\phi A_\theta\right), \\
\left(\nabla \times \vec{A}\right)_\theta &= \frac{1}{r\sin\theta} \left(\partial_\phi A_r - \sin\theta\, \partial_r (r A_\phi)\right), \\
\left(\nabla \times \vec{A}\right)_\phi &= \frac{1}{r}\, \partial_r (r A_\theta) - \frac{1}{r}\, \partial_\theta A_r,
\end{aligned}$$

$$\begin{aligned}
\left(\nabla \times \vec{A}\right)_r &= \frac{\mu_0 m_0}{4\pi} \frac{1}{r^2 \sin\theta} \left[\frac{1}{r} \cos(\omega t') - \frac{\omega}{c} \sin(\omega t') \right] \partial_\theta \sin^2\theta \\
&= \frac{\mu_0 m_0}{2\pi r^2} \cos\theta \left[\frac{1}{r} \cos(\omega t') - \frac{\omega}{c} \sin(\omega t') \right],
\end{aligned}$$

$$\left(\nabla \times \vec{A}\right)_\theta = -\frac{\mu_0 m_0}{4\pi r}\sin\theta\left[\frac{\omega}{cr}\sin\left(\omega t'\right) + \frac{\omega^2}{c^2}\cos\left(\omega t'\right) - \frac{1}{r^2}\cos\left(\omega t'\right)\right].$$

Which yields:

$$\begin{aligned}\vec{B} = &\frac{\mu_0 m_0}{2\pi r^2}\cos\theta\left[\frac{1}{r}\cos\left(\omega t'\right) - \frac{\omega}{c}\sin\left(\omega t'\right)\right]\hat{r}\\ &-\frac{\mu_0 m_0}{4\pi r}\sin\theta\left[\frac{\omega}{cr}\sin\left(\omega t'\right) + \frac{\omega^2}{c}\cos\left(\omega t'\right) - \frac{1}{r^2}\cos\left(\omega t'\right)\right]\hat{\theta}.\end{aligned}$$

A combination of spherical and Cartesian coordinates is preferred in the sense that one uses (r,x,y,z) to express the field. This choice will become clear later on, when the total field will be the superposition from fields from different coordinate systems.

$$r = \sqrt{x^2 + y^2 + z^2},$$

$$\rho = \sqrt{x^2 + y^2} = r\sin\theta,$$

$$z = r\cos\theta,$$

$$\begin{aligned}\hat{r} = \frac{x\hat{x} + y\hat{y} + z\hat{z}}{r} &= \frac{\rho}{r}\hat{\rho} + \cos\theta\,\hat{z}\\ &= \sin\theta\,\hat{\rho} + \cos\theta\,\hat{z}.\end{aligned}$$

Using these equalities one can express $\hat{\theta}$ in a more suitable manner:

$$\begin{aligned}\hat{\theta} \equiv \frac{1}{r}\frac{\partial\vec{r}}{\partial\theta} = \frac{\partial\hat{r}}{\partial\theta} &= \cos\theta\,\hat{\rho} - \sin\theta\,\hat{z}\\ &= \frac{\cos\theta}{\sin\theta}\left(\hat{r} - \cos\theta\,\hat{z}\right) - \sin\theta\,\hat{z}\\ &= \frac{1}{\sin\theta}\left(\cos\theta\,\hat{r} - \hat{z}\right).\end{aligned}$$

Alternatively one could find the unit vector from figure 4.1, where the relation between Cartesian and spherical coordinates is clearly visible. Inserted gives

$$\sin\theta\,\hat{\theta} = \frac{z}{r}\hat{r} - \hat{z}.$$

Arriving at the final expression for the magnetic field of an oscillating magnetic dipole:

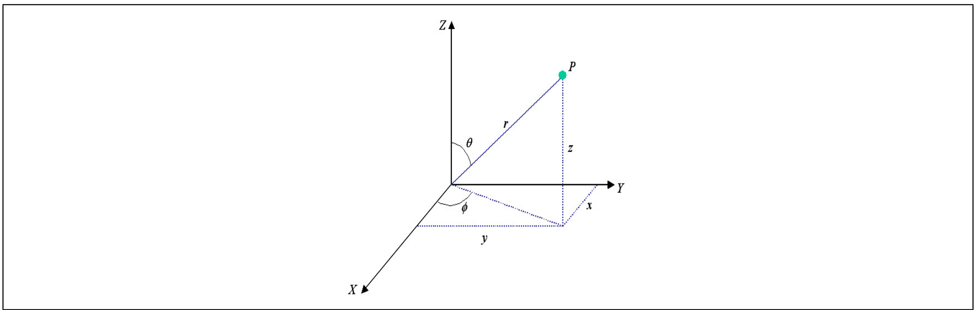

Figure 4.1: Relation between Cartesian and spherical coordinates

$$
\begin{aligned}
\vec{B} &= \frac{\mu_0 m_0}{2\pi r^2}\,\frac{z}{r}\,\left[\frac{1}{r}\cos\left(\omega t'\right)-\frac{\omega}{c}\sin\left(\omega t'\right)\right]\hat{r} \\
&- \frac{\mu_0 m_0}{4\pi r}\left[\frac{\omega}{cr}\sin\left(\omega t'\right)+\frac{\omega^2}{c^2}\cos\left(\omega t'\right)-\frac{1}{r^2}\cos\left(\omega t'\right)\right] \\
&\times\left[\frac{z}{r}\hat{r}-\hat{z}\right] \\
&= \frac{\mu_0 m_0 z}{4\pi r^2}\left[\left(\frac{3}{r^2}-\frac{\omega^2}{c^2}\right)\cos\left(\omega t'\right)-\frac{3\omega}{rc}\sin\left(\omega t'\right)\right]\hat{r} \\
&+ \frac{\mu_0 m_0}{4\pi r}\left[\left(\frac{\omega^2}{c^2}-\frac{1}{r^2}\right)\cos\left(\omega t'\right)+\frac{\omega}{rc}\sin\left(\omega t'\right)\right]\hat{z}.
\end{aligned}
$$

The next step is to find the magnetic field of a rotating magnetic dipole. Adding a second magnetic dipole perpendicular to the first one, with an angular phase shift of $\frac{\pi}{2}$, letting $\cos\theta \to \sin\theta$ and $\sin\theta \to -\cos\theta$, will do the trick. Since rotations around the z-axis is the norm the first dipole oscillates along the x-axis and the second one along the y-axis. This will result in a positive rotation in the xy-plane. However, since not all neutron stars have the magnetic axis perpendicular to the rotation axis a third magnetic static dipole in the z-direction has to be included. This one will have a strength factor λ as a variable which will allow to compute any angle between the two axes.

$$
\begin{aligned}
\vec{B}_{total} &= \frac{\mu_0 m_0}{4\pi r}\left[\left(\frac{3x}{r^3}-\frac{\omega^2 x}{c^2 r}\right)\cos(\omega t') - \frac{3\omega x}{r^2 c}\sin(\omega t')\right]\hat{r} \\
&+ \frac{\mu_0 m_0}{4\pi r}\left[\left(\frac{\omega^2}{c^2}-\frac{1}{r^2}\right)\cos(\omega t') + \frac{\omega}{rc}\sin(\omega t')\right]\hat{x} \\
&+ \frac{\mu_0 m_0}{4\pi r}\left[\left(\frac{3y}{r^3}-\frac{\omega^2 y}{c^2 r}\right)\sin(\omega t') + \frac{3\omega y}{r^2 c}\cos(\omega t')\right]\hat{r} \\
&+ \frac{\mu_0 m_0}{4\pi r}\left[\left(\frac{\omega^2}{c^2}-\frac{1}{r^2}\right)\sin(\omega t') - \frac{\omega}{rc}\cos(\omega t')\right]\hat{y} \\
&+ \frac{\lambda\cdot\mu_0 m_0}{4\pi r^2}\left(\frac{3z}{r^2}\hat{r}-\frac{\hat{z}}{r}\right) \\
&= \frac{\mu_0 m_0}{4\pi r}\left[\left(\frac{3x}{r^3}-\frac{\omega^2 x}{c^2 r}+\frac{3\omega y}{r^2 c}\right)\cos(\omega t')\right. \\
&+ \left.\left(\frac{3y}{r^3}-\frac{\omega^2 y}{c^2 r}-\frac{3\omega x}{r^2 c}\right)\sin(\omega t') + \frac{\lambda\cdot 3z}{r^3}\right]\hat{r} \\
&+ \frac{\mu_0 m_0}{4\pi r}\left[\left(\frac{\omega^2}{c^2}-\frac{1}{r^2}\right)\cos(\omega t') + \frac{\omega}{rc}\sin(\omega t')\right]\hat{x} \\
&+ \frac{\mu_0 m_0}{4\pi r}\left[\left(\frac{\omega^2}{c^2}-\frac{1}{r^2}\right)\sin(\omega t') - \frac{\omega}{rc}\cos(\omega t')\right]\hat{y} \\
&- \frac{\lambda\cdot\mu_0 m_0}{4\pi r^3}\hat{z}.
\end{aligned}
$$

The next step is to find the electric field generated by these dipoles. Using the same procedure one starts with one dipole, oscillating along the z-axis. Recall the A-field stated above:

$$
\begin{aligned}
\vec{\mathcal{E}} &= -\frac{\partial \vec{A}}{\partial t} \\
&= -\frac{\partial}{\partial t}\left(\frac{\mu_0 m_0}{4\pi}\frac{\sin\theta}{r}\left[\frac{1}{r}\cos(\omega t') - \frac{\omega}{c}\sin(\omega t')\right]\right)\hat{\phi} \\
&= \frac{\mu_0 m_0 \omega}{4\pi}\frac{\sin\theta}{r}\left[\frac{1}{r}\sin(\omega t') + \frac{\omega}{c}\cos(\omega t')\right]\hat{\phi}.
\end{aligned}
$$

The $\hat{\phi}$-vector is more practical in Cartesian coordinates. It is easier to transform Cartesian coordinates than spherical ones when changing the axis (except for the radius, which is kept intact).

$$\hat{\phi} = \frac{x\hat{y} - y\hat{x}}{\sqrt{x^2+y^2}}.$$

Using the relation $\sin\theta = \frac{\rho}{r}$ yields

$$\hat{\phi}\sin\theta = \frac{x\hat{y} - y\hat{x}}{r}.$$

Inserting and transforming allows to get the rotating dipole. The electric field becomes:

$$\begin{aligned}\vec{\mathcal{E}}_{total} = &\frac{\mu_0 m_0 \omega}{4\pi r^2}\left[\frac{1}{r}\sin\left(\omega t'\right) + \frac{\omega}{c}\cos\left(\omega t'\right)\right] \times \left[y\hat{z} - z\hat{y}\right] \\ &+ \frac{\mu_0 m_0 \omega}{4\pi r^2}\left[-\frac{1}{r}\cos\left(\omega t'\right) + \frac{\omega}{c}\sin\left(\omega t'\right)\right] \times \left[z\hat{x} - x\hat{z}\right].\end{aligned}$$

It is now possible to find the Lorentz force acting on a charged particle rotating with the star. Its velocity term will be of the form:

$$\vec{v} = \rho\omega\hat{\phi} = \omega\left(x\hat{y} - y\hat{x}\right),$$

where ϕ is given from the frame of the rotating dipole. The B-field is of the form $\alpha\hat{x} + \beta\hat{y} + \sigma\hat{z} + \gamma\hat{r}$, which yields

$$\begin{aligned}\vec{v} \times \vec{B} &= \omega\left(x\hat{y} - y\hat{x}\right) \times \left[\alpha\hat{x} + \beta\hat{y} + \sigma\hat{z} + \gamma\hat{r}\right] \\ &= \omega\sigma x\hat{x} + \omega\sigma y\hat{y} - \omega\left(\alpha x + \beta y\right)\hat{z} + \rho\omega\gamma\hat{\theta}.\end{aligned}$$

Rewriting the $\hat{\theta}$-vector

$$\begin{aligned}\hat{\theta} &= \frac{1}{\sin\theta}\left(\frac{z}{r}\hat{r} - \hat{z}\right) \\ &= \frac{z}{\rho}\hat{r} - \frac{r}{\rho}\hat{z} \\ &= \frac{z}{\rho r}(x\hat{x} + y\hat{y} + z\hat{z}) - \frac{r}{\rho}\hat{z} \\ &= \frac{z}{\rho r}(x\hat{x} + y\hat{y}) - \frac{r^2 - z^2}{\rho r}\hat{z} \\ &= \frac{z}{\rho r}(x\hat{x} + y\hat{y}) - \frac{\rho}{r}\hat{z}\end{aligned}$$

Emplpoying the new $\hat{\theta}$-vector, the Lorentz force can be expressed:

$$\begin{aligned}\vec{F}_{Lorentz} &= q\left(\vec{\mathcal{E}} + \vec{v} \times \vec{B}\right) \\ &= q\begin{bmatrix}\mathcal{E}_x + \omega x\sigma + \frac{zx\omega\gamma}{R} \\ \mathcal{E}_y + \omega y\sigma + \frac{zy\omega\gamma}{R} \\ \mathcal{E}_z - \omega\left(\alpha x + \beta y\right) - \frac{\rho^2\omega\gamma}{R}\end{bmatrix},\end{aligned}$$

where the components $\mathcal{E}_x$, $\mathcal{E}_y$, $\mathcal{E}_z$, α, β, γ and σ are defined below:

$$\mathcal{E}_x = \frac{\mu_0 m_0 \omega}{4\pi R^2}\left(\frac{\omega}{c}\sin(\omega t') - \frac{1}{r}\cos(\omega t')\right)z,$$

$$\mathcal{E}_y = -\frac{\mu_0 m_0 \omega}{4\pi R^2}\left(\frac{1}{r}\sin(\omega t') + \frac{\omega}{c}\cos(\omega t')\right)z,$$

$$\mathcal{E}_z = \frac{\mu_0 m_0 \omega}{4\pi R^2}\left[\left(\frac{1}{r}\sin(\omega t') + \frac{\omega}{c}\cos(\omega t')\right)y + \left(\frac{1}{r}\cos(\omega t') - \frac{\omega}{c}\sin(\omega t')\right)x\right],$$

$$\alpha = \frac{\mu_0 m_0}{4\pi r}\left[\left(\frac{\omega^2}{c^2} - \frac{1}{r^2}\right)\cos\left(\omega t'\right) + \frac{\omega}{rc}\sin\left(\omega t'\right)\right],$$

$$\beta = \frac{\mu_0 m_0}{4\pi r}\left[\left(\frac{\omega^2}{c^2} - \frac{1}{r^2}\right)\sin\left(\omega t'\right) - \frac{\omega}{rc}\cos\left(\omega t'\right)\right],$$

$$\sigma = -\frac{\lambda \cdot \mu_0 m_0}{4\pi r^3},$$

$$\gamma = \frac{\mu_0 m_0}{4\pi r}\left[\left(\frac{3x}{r^3} - \frac{\omega^2 x}{c^2 r} + \frac{3\omega y}{r^2 c}\right)\cos\left(\omega t'\right) + \left(\frac{3y}{r^3} - \frac{\omega^2 y}{c^2 r} - \frac{3\omega x}{r^2 c}\right)\sin\left(\omega t'\right) + \frac{\lambda \cdot 3z}{r^3}\right].$$

The expanded force vector is a long equation, which does not give more insight than the form above. The expanded version is given in appendix B.

Magnetic field on neutron stars is of the order 10^8T, and the magnetic field constructed is of the order:

$$B \simeq \frac{\mu_0 m_0}{2\pi r^2}\left(\frac{1}{r} + \frac{\omega}{c}\right) \simeq 10^8\text{T}.$$

Inserting the values $R = 10^4$m and $\omega \simeq 10^3$ one obtains

$$\mu_0 m_0 \simeq 10^{21}\text{Tm}^3.$$

The order of magnitude of the force on an electron corotating on the equator of the star becomes

$$\begin{aligned}\|\vec{F}_{Lorentz}(R,0,0)\| &\simeq q\frac{\mu_0 m_0 \omega}{4\pi R^2} \\ &\simeq 10^{-4}\text{N}.\end{aligned}$$

For comparison the gravitational force on the same electron is

$$\begin{aligned}\|\vec{F}_g\| &= G\frac{m_e M_{NS}}{R^2} \\ &= 6.67 \cdot 10^{-11}\frac{9.1 \cdot 10^{-31} \cdot 1.4 \cdot 2.0 \cdot 10^{30}}{10^8} \\ &= 1.7 \cdot 10^{-18}\text{N}.\end{aligned}$$

4.1 Numerical simulations

In order to simulate the Lorentz force on a charged particle, all star dependent variables have to be set. The Crab pulsar is the second youngest pulsar in the universe, after Kes 75, less than 1000 years old meaning it has more energy left than other older alternatives. It is also one of the most studied and known pulsar. Hence it is an excellent candidate for the simulations. The magnetic field is estimated to be $B = 4 \cdot 10^8$ T, the radius is $1.00 \cdot 10^4$m and the period $33 \cdot 10^{-3}$s. The force on an electron is chosen. The strongest field is given by:

$$\|\vec{B}\| \approx \frac{\mu_0 m_0}{2\pi r^3} = 4 \cdot 10^8 \text{ T}.$$

$$\begin{aligned} \Rightarrow \mu_0 m_0 &= 2\pi \cdot 10^{12} \cdot 4 \cdot 10^8 \\ &= 8\pi \cdot 10^{20} \\ &= 2.5 \cdot 10^{21}. \end{aligned}$$

Using matlab simulations Lorentz force on the electron at the surface is found and mapped. A spherical coordinate system (r, ϕ, θ) is used, as commonly used in physics, with radius r, azimuth angle ϕ and polar angle θ. The polar angle θ has zero value at the equator. All plots are made in phase. The normal force components are indicated with colors while the tangential components correspond to the vector arrows. All forces are in newton. The mapping does not conserve length as length along ϕ-direction is θ dependent. Nevertheless, the vector arrows are all at scale to the felt force. Since the mapping does not conserve length in the ϕ-direction, angles become distorted in the transformation from the surface of the star to the plot. In order to compensate the direction of the vectors have been altered: in the xy-plane, where the y-axis corresponds to the θ-axis and the x-axis to the ϕ-axis, a vector $\vec{v} = a\hat{x} + b\hat{y}$ transforms as:

$$\vec{v} \Rightarrow \vec{v}' = n \cdot a\hat{x} + n\frac{b}{\sin\theta}\hat{y},$$

where n is given as

$$n = \frac{\sqrt{a^2 + b^2}}{\sqrt{a^2 + b^2 \sin^2\theta}},$$

letting the vector transformation preserve length, but alter the angle such that the transformed angle will correspond to the angle on the surface of the star. Only the Lorentz force has been plotted, which is practically equal to the total force on the particle, as will be seen later in section 4.2.

Until now only forces in the inertial frame have been examined. But since the rotating frame is not an inertial reference frame one cannot simply use a Lorentz transform. Changing to a rotating field one has to take into account the fictitious *centrifugal* force and the *Coriolis* force. However, since the test particle is at rest on the star surface the Coriolis force does not affect it. The centrifugal force is expressed

$$
\begin{aligned}
\|\vec{F}_{centrifugal}\| = \|\vec{\omega} \times (\vec{\omega} \times \vec{r})\, m_e\| &\leq \omega^2 R m_e \\
&\leq 190^2 \cdot 10^4 \cdot 9.1 \cdot 10^{-31} \\
&\leq 3.29 \cdot 10^{-22}\ \text{N}.
\end{aligned}
$$

Hence all other forces are many orders of magnitude weaker than the Lorentz force in the inertial frame. Since the centrifugal is negligible the Lorentz force is the same in both the inertial frame and in the corotating frame.

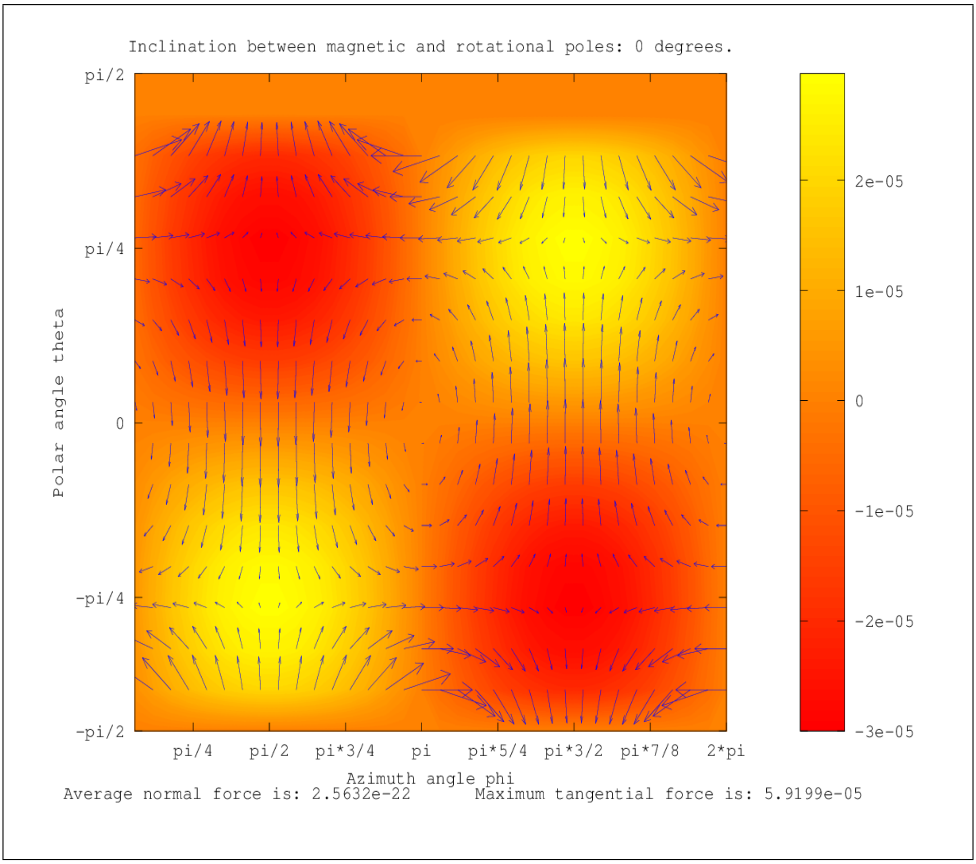

Figure 4.2: Lorentz force on a corotating electron with magnetic poles inclined at $\theta = 0$ from the equator.

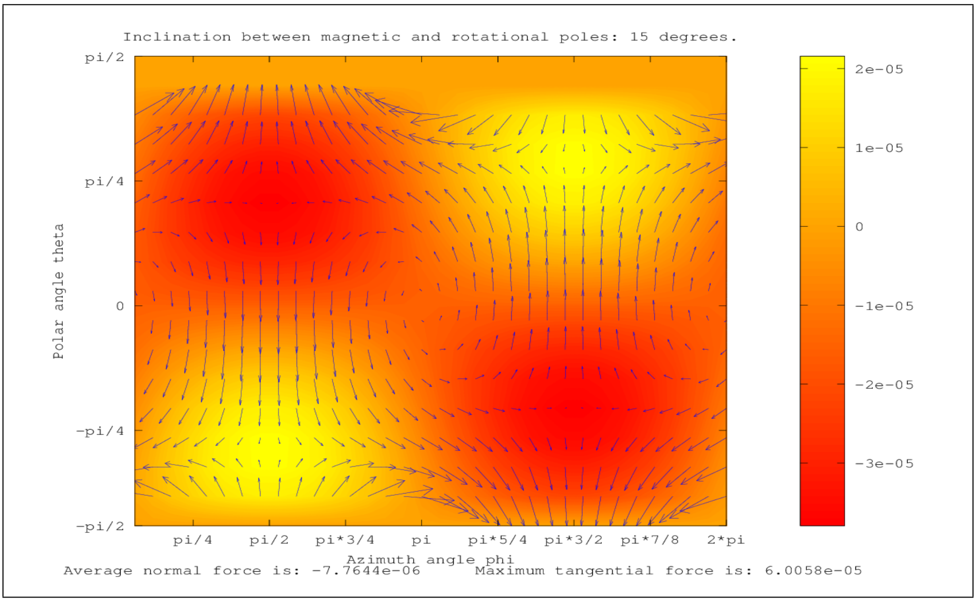

Figure 4.3: Lorentz force on a corotating electron with magnetic poles inclined at $\theta = \frac{\pi}{12}$ from the equator.

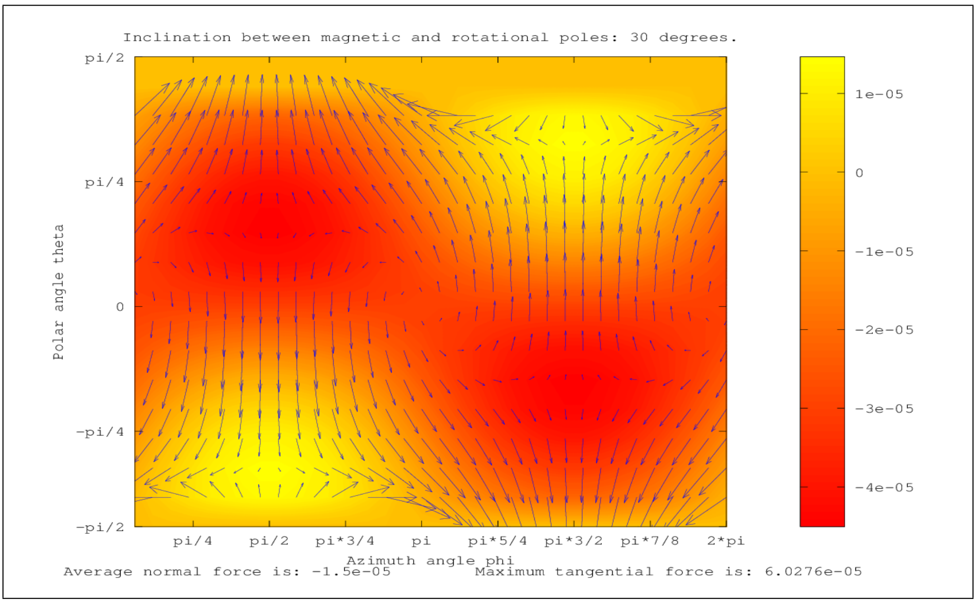

Figure 4.4: Lorentz force on a corotating electron with magnetic poles inclined at $\theta = \frac{\pi}{6}$ from the equator.

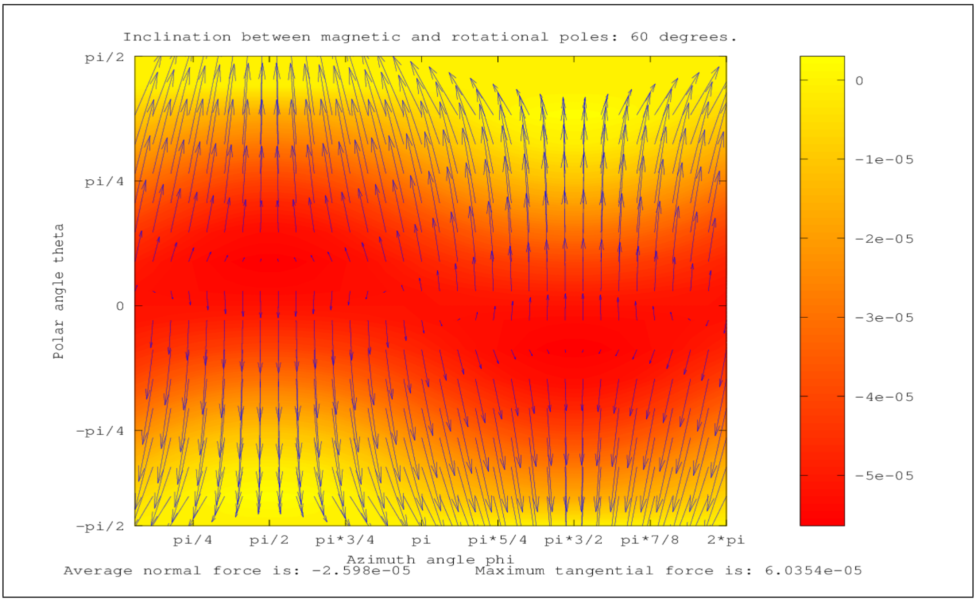

Figure 4.5: Lorentz force on a corotating electron with magnetic poles inclined at $\theta = \frac{\pi}{3}$ from the equator.

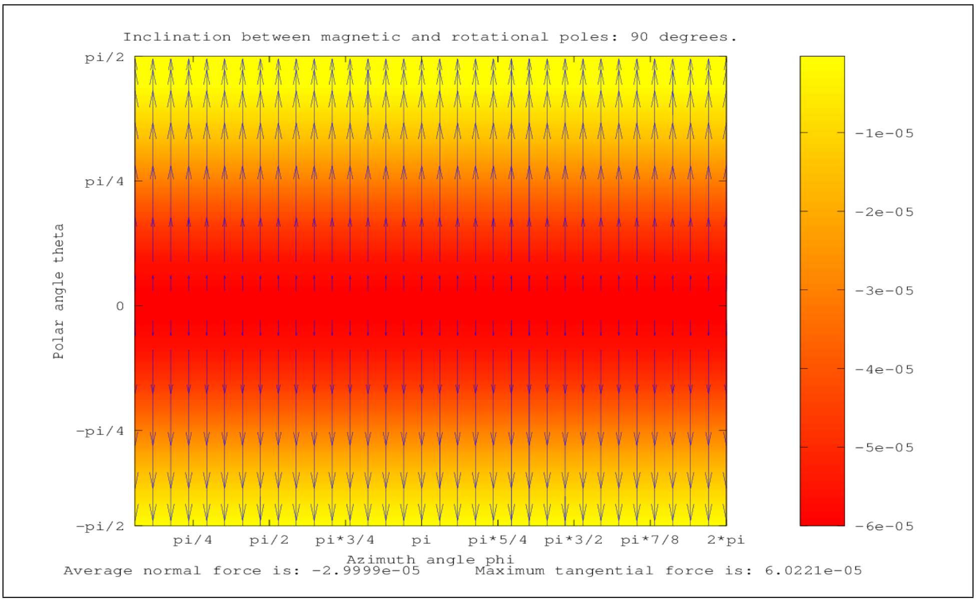

Figure 4.6: Lorentz force on a corotating electron with magnetic poles inclined at $\theta = \frac{\pi}{2}$ from the equator.

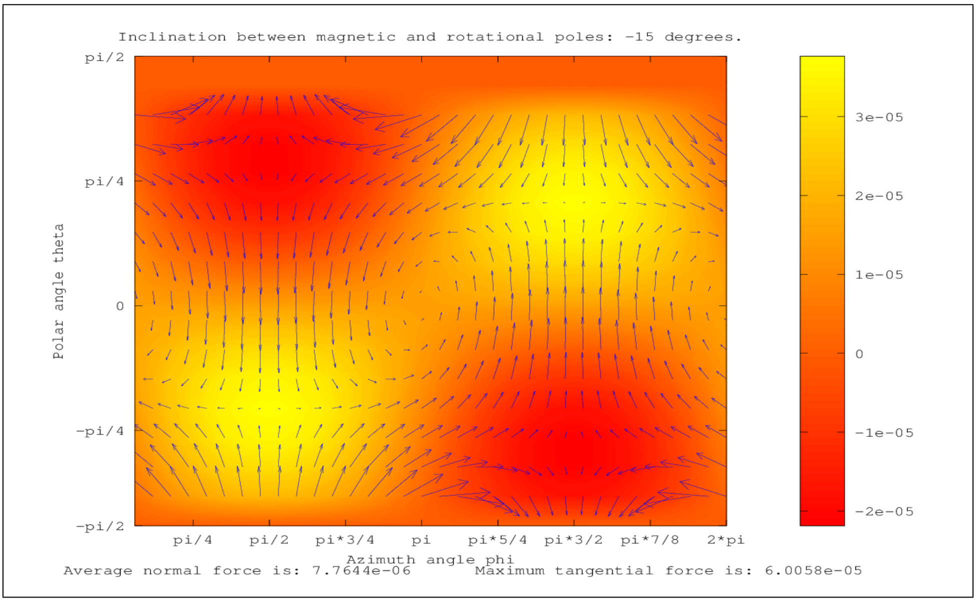

Figure 4.7: Lorentz force on a corotating electron with magnetic poles inclined at $\theta = -\frac{\pi}{12}$ from the equator.

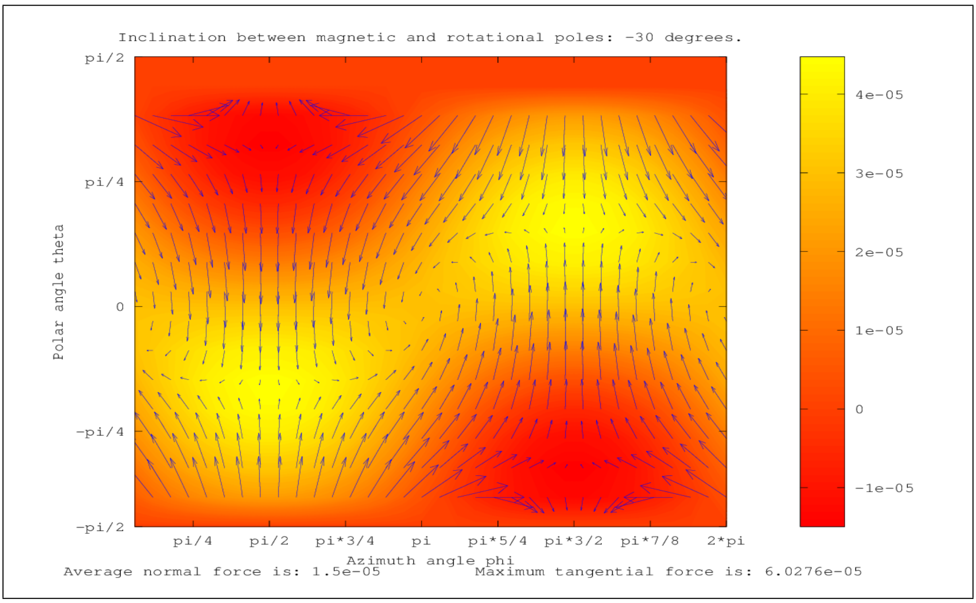

Figure 4.8: Lorentz force on a corotating electron with magnetic poles inclined at $\theta = -\frac{\pi}{6}$ from the equator.

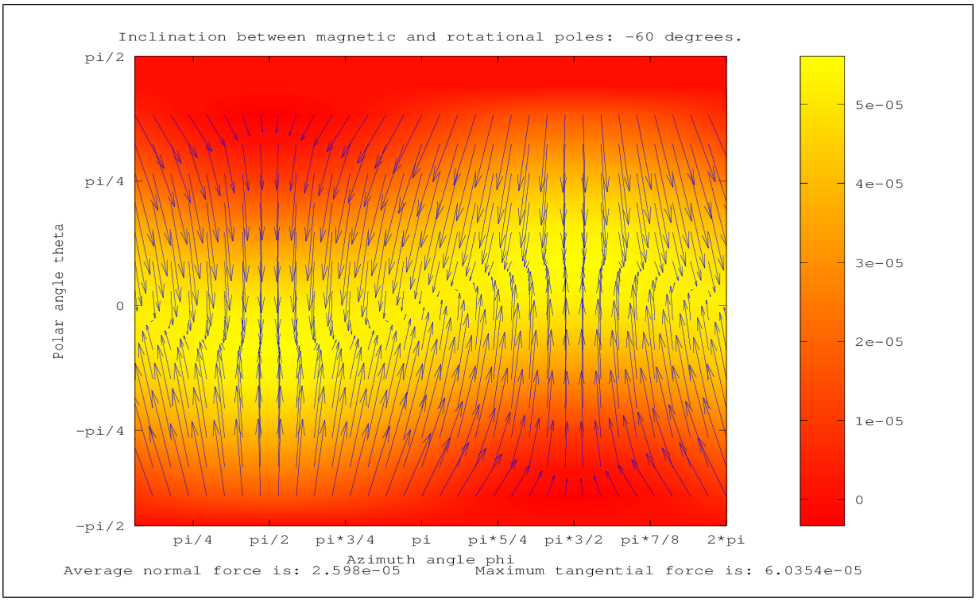

Figure 4.9: Lorentz force on a corotating electron with magnetic poles inclined at $\theta = -\frac{\pi}{3}$ from the equator.

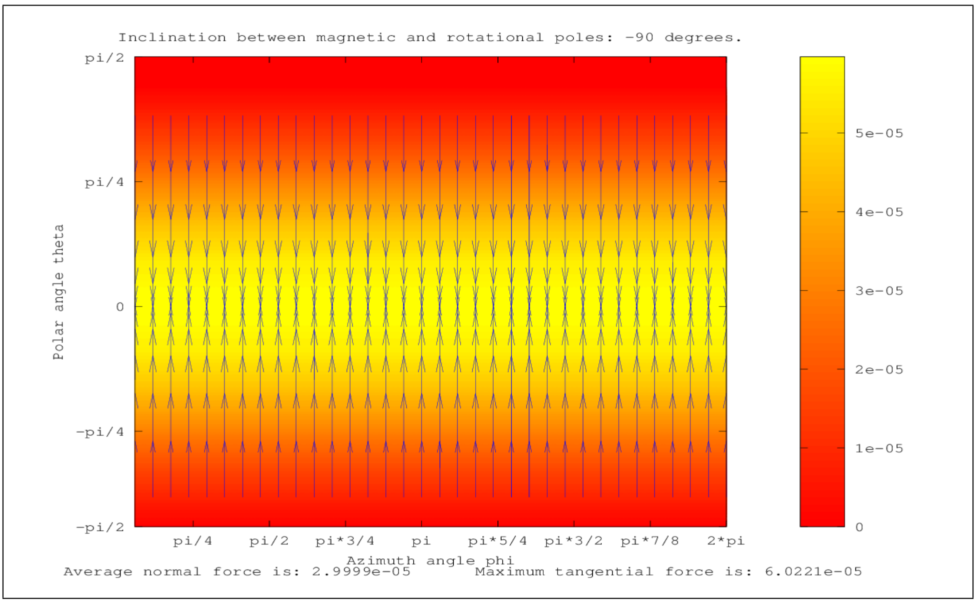

Figure 4.10: Lorentz force on a corotating electron with magnetic poles inclined at $\theta = -\frac{\pi}{2}$ from the equator.

4.1.1 Discussions

As the Lorentz force is the same in both frames and the test particle is at rest in the rotating frame only an effective electric field $\vec{\vec{\mathcal{E}}} = \vec{\mathcal{E}} + \vec{v} \times \vec{B}$ will affect the test particle. A contribution from the $\vec{v} \times \vec{B}$ means the two different electric fields are different, this does not mean the charge is different in the frames, as charge is *Lorentz invariant*.

Magnetic poles along the equator

In figure 4.2 the effective normal electric field takes the form of a central symmetric quadrupole, while the tangential field flows around several vortices. The field is anti-symmetric with respect to a plane cutting through the star at the middle of the map, at $\theta = 0, \pi$, and anti-symmetric with respect to the equatorial plane. The tangential forces follow a circular flow around two strong vortex on the equator, and two strong dipole vortex on the rotational poles. The tangential and normal forces are of the same order and the average normal force is zero.

Magnetic poles between the equator and the rotational poles

In figures 4.3, 4.4, 4.5, 4.7, 4.8 and 4.9 the magnetic poles are inclined between the rotational poles and the equator. The more inclined the magnetic poles are compared to the equator, the more the quadrupole landscape vanishes. The peaks move: in the case where the inclination angle is positive the negative peaks move towards the equator while the positive ones move towards the rotational poles. The average normal force also changes: for positive inclination angles, the average force is negative, and if the inclination angle is negative the average force is positive. The average normal force increases in absolute value as the angle increases in absolute value. Which means the effective field is not only constituted by a quadrupole but also at least a monopole. The peaks move relatively to each other, the negative poles are closer to the equator in the case of positive inclination angles, meaning that the anti-symmetry mentioned in section 4.1.1 about the plane at $\theta = 0, \pi$ is broken, but the one with respect to the equatorial plane is conserved. All of the vortex become weaker as the inclination increases, with no vortex at all when the poles are aligned.

Magnetic and rotational poles aligned

In figures 4.6 and 4.10 the magnetic poles are aligned with the rotational poles. Hence there is no magnetic oscillation and the field is time independent in the inertial reference frame. At the poles there is no net force, and the force increases as the particle closes to the equator. In the case of positive inclination angle the equator is a negative peak, with tangential flows flowing towards the nearest pole.

Changing the charge sign, equivalent to changing to a proton, changes the sign of the force. Even though the proton mass is close to 2000 times the electron's the electromagnetic forces are still much stronger than the gravitational force, so one would expect a very close similarity between the electron distribution and the proton distribution in the strong electromagnetic fields. One would expect electrons to flow together and stack at the peaks, and protons to flow in the opposite direction. At the normal force peaks electrons and protons will be either pushed or pulled off the surface, in opposite direction of one another.

Remarks

This model is of course not very accurate since particles are assumed to be at rest on the star's surface, but assuming the motion of particles does not affect the forces significantly it can still provide valuable information. Such strong forces would deform the spherical shape of the star creating mountains on the order of meters around the poles. Indeed this idea has already been explored[16]. If these mountains are high enough while the spin rate is high, *gravitational waves* will be emitted due to the gained inertial quadrupole momentum. Dissipating energy through gravitational waves will in turn reduce the spin energy and slow down the spin of the star. Another possible implication is the stacking and flows of charged particles will in turn counter the strong electromagnetic forces, creating opposite electric and magnetic fields, taking the form of an opposite field as the one mapped.

4.2 Electric field inside the neutron star

The next step is to look at the forces on particles at rest in the corotating frame. Letting the gravity term incorporate the centripetal force component, one gets one electric field component and one gravity component. Only the presence of electrons, neutrons and protons is assumed, and the Fermi sphere as Equation of State at zero temperature is used:

$$\vec{g} = -g\vec{e}_z,$$
$$\vec{\mathcal{E}} = \mathcal{E}\vec{e}_z.$$

Where the z-axis is the vertical axis with the unit vector pointing outwards. $\mathcal{E}$ is the electric field strength, and must not be confused with ϵ_0, which is the vacuum permittivity. Using the identities:

$$\nabla \cdot \vec{g} = -\frac{\mathrm{d}g}{\mathrm{d}z} = -4\pi G\rho_m,$$
$$\nabla \cdot \vec{\mathcal{E}} = \frac{\mathrm{d}\mathcal{E}}{\mathrm{d}z} = \frac{\rho_q}{\epsilon_0},$$

where ρ_m is the mass density and ρ_q the charge density. The mass is the number density times the mass of electrons, protons and neutrons, whereas the charge density is the number density times charge for electrons and protons.

$$\frac{\mathrm{d}g}{\mathrm{d}z} = 4\pi G(m_p n_p + m_n n_n + m_e n_e),$$
$$\frac{\mathrm{d}\mathcal{E}}{\mathrm{d}z} = \frac{e}{\epsilon_0}(n_p - n_e),$$

where e is the elementary charge. The number density in a Fermi sphere is given by:

$$n_e = \frac{8\pi}{3h^3}p_F^3.$$

The density for protons and neutrons is similar, changing the electron index e to n or p. The relativistic Fermi energy is given by:

$$E_F = \sqrt{m^2c^4 + p_F^2c^2}.$$

In order to find the energy derivative:

$$E_F^2 = m^2c^4 + p_F^2c^2,$$

$$\Rightarrow 2E_F\frac{\mathrm{d}E_F}{\mathrm{d}z} = 2p_F\frac{\mathrm{d}p_F}{\mathrm{d}z}. \tag{4.1}$$

The total energy variation is the contribution from the electric force and from the gravitational force:

$$\frac{\mathrm{d}E_{Fp}}{\mathrm{d}z} = -m_pg + e\mathcal{E}, \tag{4.2}$$

$$\frac{\mathrm{d}E_{Fe}}{\mathrm{d}z} = -m_eg - e\mathcal{E}. \tag{4.3}$$

The factor $\frac{8\pi}{3h^3} = 2.8 \cdot 10^{100}$ J^{-3}s^{-3} connecting the number density and Fermi momentum is huge, meaning a small difference in momentum between $p_{F,e}$ and $p_{F,p}$ has enormous consequences for the $\mathcal{E}$-field. Hence the equality $p_{F,e} = p_{F,p}$ holds to large orders of accuracy. Inducing the equality $\frac{\mathrm{d}p_{Fp}}{\mathrm{d}z} = \frac{\mathrm{d}p_{Fe}}{\mathrm{d}z}$. Employing the last identity and using equation 4.1 yields

$$E_{Fp}\frac{\mathrm{d}E_{Fp}}{\mathrm{d}z} = E_{Fe}\frac{\mathrm{d}E_{Fe}}{\mathrm{d}z}.$$

Inserting the formulas 4.2 and 4.3 yields

$$E_{Fp}\left(-m_pg + e\epsilon\right) = E_{Fe}\left(-m_eg - e\mathcal{E}\right).$$

Rearranging and solving for $e\mathcal{E}$:

$$\begin{aligned} e\mathcal{E} &= \frac{E_{Fp}m_p - E_{Fe}m_e}{E_{Fp} + E_{Fe}}g \\ &= \frac{m_p^2c^2 - m_e^2c^2}{m_pc^2 + m_ec^2}g \\ &= \left(m_p - m_e\right)g, \end{aligned}$$

where p_F goes to zero since the surface is reached. where the energy is expanded to zeroth order: $p_F \to 0$, hence

$$\begin{aligned} \mathcal{E} &= \frac{m_p - m_e}{q}g \\ &= \frac{1.6 \cdot 10^{-27}\text{kg}}{1.6 \cdot 10^{-19}\text{C}} \cdot 2 \cdot 10^{12}\text{m/s}^2 \\ &= 2 \cdot 10^4\text{V/m}, \end{aligned}$$

is the electric field necessary to keep charge neutrality near the surface. Which is a very unusual effect, as one is taught in every course in electromagnetism that conductors do not allow electric fields inside. But this effect takes place due to the powerful gravitation, which one never encounters in basic electromagnetism. The value of g combines the centrifugal and gravitational forces:

$$\begin{aligned} F = mg &= G\frac{mM_{NS}}{R^2} - m\omega^2 R \\ \Rightarrow g &= G\frac{M_{NS}}{R^2} - \omega^2 R \\ &= 6.67 \cdot 10^{-11}\frac{1.44 \cdot 1.99 \cdot 10^{30}}{10^8} - 190^2 \cdot 10^4 \\ &= 1.91 \cdot 10^{12} - 3.61 \cdot 10^8 \\ &\simeq G\frac{M_{NS}}{R^2} = 1.91 \cdot 10^{12}, \end{aligned}$$

which implies the centrifugal force can be neglected

4.2.1 Charge density near the surface

The aim of this section is to find the equation which will be computed in C++. Hence, the angle of view will be a bit different from the previous section, but the general procedure is identical. As found earlier the electric field around the stars is strong. As the neutron star is a superconductor there can be no fields inside the star (except the one found in the previous subsection keeping the charge neutrality). Hence the fields outside must come from charges on, or very close to, the surface.

Assuming surface charges is the answer is the easiest. Recalling equation 3.6:

$$\sigma = \epsilon_0 \mathcal{E},$$

According to the previous sections the strongest forces acting on an electron are of the order $2 \cdot 10^{-5}$N.

$$\begin{aligned} \sigma_{max} &= \epsilon_0 \frac{F_{max}}{e} \\ &= 8.854 \cdot 10^{-12}\frac{2 \cdot 10^{-5}}{1.602 \cdot 10^{-19}} \\ &= 1.10 \cdot 10^3 \text{ C/m}^2. \end{aligned}$$

Which is a high charge concentration. To assume the charges are only at the surface is a bold assumption. It is much more physical to assume the charges spread beneath the surface. Using a degenerate gas as EoS in a sphere in a static situation in the sense that particles are at rest yields: The total number of electrons:

$$N_e = 2 \cdot v\frac{4\pi}{3}p_{Fe}^3,$$

where the 2 factor comes from both spin directions.

$$n_e = \frac{N_e}{v} = \frac{8\pi}{3} p_{Fe}^3. \tag{4.4}$$

Expressing the relativistic momentum with the energy:

$$E_{Fe} = \sqrt{m_2^2 c^4 + p_{Fe}^2 c^2}.$$

In order to gain accuracy in the computer simulations a transformation is needed:

$$\begin{aligned} E_{Fe}^2 - m_e^2 c^4 &= (\underbrace{E_{Fe} - m_e c^2}_{E_{ke}})(E_{Fe} + m_e c^2) \\ &= E_{ke}(E_{ke} + 2mc^2). \end{aligned}$$

where the subindex k stands for kinetic. Employing the transformation the momentum becomes

$$\begin{aligned} p_{Fe} &= \sqrt{\frac{E_{Fe}^2}{c^2} - m_e^2 c^2} \\ &= \sqrt{\frac{E_{ke}(E_{ke} + 2m_e c^2)}{c^2}}. \end{aligned} \tag{4.5}$$

The region near the surface is the main area of interest meaning simplifications are possible: gravity can be looked as linear. The system is now one dimensional with the z-axis in radial direction.

$$E_{Fe} = E_{Fe}^0 - m_e g z - q_e \phi(z). \tag{4.6}$$

All of the formulas above have an equivalent version for protons.

According to *Gauss' law* the field can be written:

$$\begin{aligned} \nabla \cdot \vec{\mathcal{E}} &= \frac{\rho}{\epsilon_0} \\ &= \frac{1}{\epsilon_0} \left(q_e n_e + q_p n_p \right), \end{aligned}$$

writing using the scalar potential instead $\vec{\mathcal{E}} = -\nabla \phi$ yields

$$\boxed{\nabla^2 \phi(z) = -\frac{1}{\epsilon_0} \left(q_e n_e + q_p n_p \right)} \tag{4.7}$$

Inserting equations 4.4, 4.5 and 4.6 into equation 4.7 yields the final expression

$$\begin{aligned} \nabla^2 \phi = &\left[(E_e^0 - m_e g z - q_e \phi - m_e c^2)(E_e^0 - m_e g z - q_e \phi + m_e c^2) \right]^{3/2} \\ &- \left[(E_p^0 - m_p g z - q_p \phi - m_p c^2)(E_p^0 - m_p g z - q_p \phi + m_p c^2) \right]^{3/2}. \end{aligned}$$

Numerical simulations

Finding a ϕ satisfying the differential equation would give the electric field and hence the charge distribution, which one expects should be very strong near the surface and decaying exponentially going under the star surface. In order to find the solution to the differential equation $y'' = f(x, y)$, the third order *Runge-Kutta Method* was employed in C++. With boundary conditions $\mathcal{E} = -\frac{\partial \phi}{\partial z} = 0$ at the bottom position of 50m under the star surface and $\mathcal{E} = -\frac{\partial \phi}{\partial z} = \frac{1}{q}10^{-5} \simeq 10^{14}$ V/m, found in the numerical simulations from section 4.1, where the electric force is of the order of 10^{-5} N, as top position, of 50m above the surface.

However, this differential equation turned out to be unsolvable, it diverged very rapidly due to the enormous factor $\frac{8\pi}{3h^3}$. A slight difference between n_p and n_e escalates into a divergent $\mathcal{E}$-field. The equation was a stiff differential equation. But the insolvability has implications.

4.2.2 Remarks

One of the assumptions done in the simulations from section 4.1 is that this is a static situation with no particle flux. With such strong electromagnetic forces acting on the electrons they will be ripped out of the surface in an atmosphere of plasma, known as the *electrosphere*.

4.3 The electrosphere

Due to the strong electromagnetic fields charged particles get ripped out of the surface near the poles. These particles form a layer of plasma inside the magnetosphere called the *electrosphere*. This low density layer ($n = 10^{17}$ m^{-3}) is dictated by the field lines, with particles following the field lines from one pole to the other, creating a corotating layer, even overrotating to a factor of three, layer of plasma. Some of the field lines are open, since they leave the light cylinder as in figure 4.11. Particles following these field lines get ejected as a *jet*. As particles follow the field lines they emit synchroton radiation, which is observed in the X-rays spectrum. In figure 4.12, the jet, the electrosphere and the surrounding matter of the Crab pulsar are visible as they emit radiation. For more details see the the lecture notes from Jérôme Pétri[15].

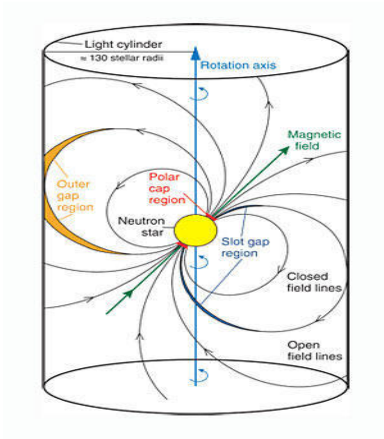

Figure 4.11: A neutron star inside the cylinder with radius $r = \frac{c}{\omega}$. The field lines are shown, both the closed ones and the open ones going out of the cylinder.

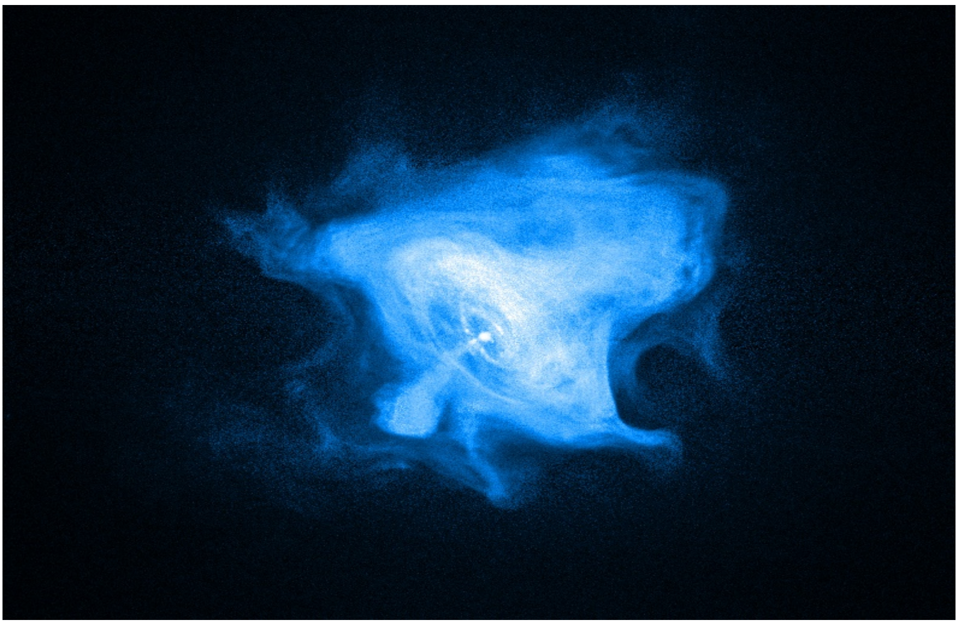

Figure 4.12: The Crab pulsar observed in X-rays, taken by NASA's Chandra X-ray Observatory[13]. The pulsar is visible as the bright dot in the center, with two outgoing jets. The surrounding plasma is powered by the magnetic field of the pulsar.

Chapter 5

Conclusion and outlook

Neutron stars show a large variety: between the young fast radio pulsars, the magnetically strong magnetars and accreting pulsars to the millisecond pulsars that have stopped accreting. All of them share a great gravitational force dominating their shape. However, in the case of the fast and magnetically strong pulsars the electromagnetic forces dominate over the gravity on the charged particles creating flows, an electrosphere and even possibly magnetically confined mountains. Being the most compact objects observable in the universe, while exhibiting different extreme characteristics, they are one of the most important laboratories for unveiling new physics: behavior in strong gravitational fields, the nuclear physics in such high densities, gravitational waves etc... Indeed, it is a hot topic. This thesis gave a short introduction to the vast topic of neutron stars before narrowing down on a simple model of the magnetic field an its implication on charges. Difficult and unresolved issues as the EoS are not encountered in the second part, as only classical electromagnetism and SR are used. The open and vague subject and technical difficulties with the simulations slowed the work. The idea of an induced quadrupole working against the ones found is an interesting idea, which unfortunately could not be included in this thesis and thus paving the way for further research possibilities, belonging in the outlook section. The idea of continuing to work on the subject after the thesis has been handed in has been discussed with the supervisor, with the induced quadrupole as topic. Two other objectives belong in the outlook section: The charge density near the surface, which the student was not able to find, is a task which should be done. In order to do so a different procedure should be employed, as the one used did not succeed. A possible approach would be to use solid state physics. Another interesting point which could be characterized as outlook is a model including particle motions. The problem immidiately becomes more complicated, and in order to restrain the complexity the flows should only be at the surface, which will let the difficult topic of the EoS be untouched.

Bibliography

[1] http://www.astro.soton.ac.uk/ mjc/res/hmxb.html.

[2] http://www.spacetimetravel.org/galerie/bnm-0251.png.

[3] Lecture notes, Cornell University.

[4] Bending of light in schwarzschild geometry. Lecture notes, Reed college, Oregon, USA.

[5] Patruno A. and Watts A.L. Accreting millisecond x-ray pulsars. arXiv:1206.2727 [astro-ph.HE].

[6] B.W. Carroll and D. A. Ostlie. *An introduction to modern astrophysics*. Pearson internation edition, second edition, 2007.

[7] X.H. Cui, H.G. Wang, and G.J. Qiao. Pulsar kicks and γ-ray burst. *Astronomy and Astrophysics*, 2007.

[8] P.P. Eggleton. Approximations to the radii of roche lobes. *Astrophysical Journal*, 1982.

[9] B. Gaensler and F. Dale. Some stars may be older than they look. *Nature*, 2000.

[10] D.J. Griffiths. *Introduction to Electrodynamics*. Pearson international edition, third edition, 2008.

[11] J.M. Lattimer and A. Burrows, 1986.

[12] C. Miller. Lecture notes in Accretion.

[13] NASA. www.nasa.gov.

[14] A. Patruno. *Accreting millisecond X-ray pulsars, from accretion disk to magnetic poles*. 2009.

[15] J. Pétri. Electrodynamics of neutron star magnetospheres. Centre dÉtude des Environnements Terrestre et Planétaires, Laboratoire de Radio Astronomie, École Normale Supérieure, France.

[16] M. Priymak, A. Melatos, and D.J.B. Payne. Quadrupole moment of a magnetically confined mountain on an accreting neutron star: effect of the equation of state. 2011. arXiv:1109.1040.

[17] Knoxville University of Tennessee. Lecture notes: Conductors in electrostatics.

Appendix A

Roche Lobe

This appendix follows the thread of an article. For further details see the article[8]. In a binary system there are two gravitational poles. The region of space around one of the stars in this system where orbiting matter is gravitationally bound to that star is called the *Roche lobe*. In a binary system with a neutron star and a companion star the companion will often expand past its Roche lobe. At that point matter will escape the gravitational pull of the companion and fall in through the inner Lagrangian point onto the accretion disc of the neutron star. This process is referred to as *mass transfer via Roche-lobe overflow*. The evolution of the mass transfer depends of the companion star's mass.

The precise shape of the Roche lobe depends on the respective masses, and must be evaluated numerically. It is however useful to approximate the Roche lobe as a sphere with the same volume, with radius:

$$r_r = \frac{0.49q^{2/3}}{0.6q^{2/3} + \ln(1 + q^{1/3})},$$

where $r_r = \frac{r}{A}$ is the effective radius of a Roche lobe, r the studied star's radius, A the semi-major axis of the system and $q = \frac{M_1}{M_2}$ the mass ratio between the binaries two masses with the studied mass as M_1. This approximation is accurate up to 1% over the entire range of q.

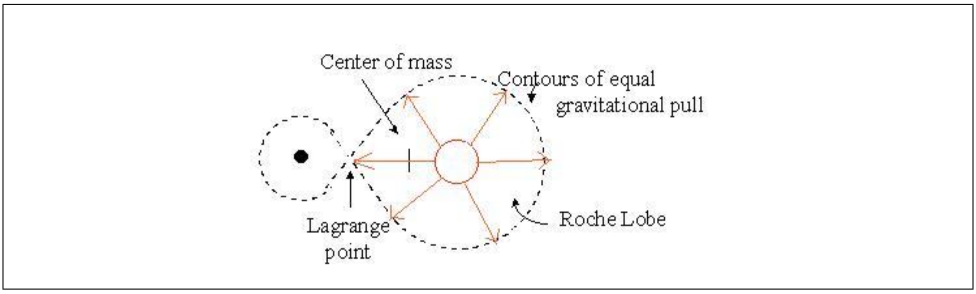

Figure A.1: Roche lobe, as seen as the dotted surface around the companion star. As the Roche lobe is full, mass will fall onto the neutron star through the Lagrange point[3].

Appendix B

Expanded Lorentz force

$$
\begin{aligned}
\vec{F}_{Lorentz} = q \Bigg(& \Bigg(\left(\frac{\mu_0 m_0 \omega}{4\pi} \, \frac{1}{r^2} \left(\left[\frac{1}{r} \sin(\omega t') + \frac{\omega}{c} \cos(\omega t') \right] y \right. \right. \\
& - \left. \left[-\frac{1}{r} \cos(\omega t') + \frac{\omega}{c} \sin(\omega t') \right] x \right) \\
& + \frac{\omega \mu_0 m_0}{4\pi r^2} \left[-\left(x^2 + y^2\right) \left[\left(\frac{3x}{r^3} - \frac{\omega^2 x}{c^2 r} + \frac{3\omega y}{r^2 c} \right) \cos(\omega t') \right. \right. \\
& + \left. \left(\frac{3y}{r^3} - \frac{\omega^2 y}{c^2 r} - \frac{3\omega x}{r^2 c} \right) \sin(\omega t') + \frac{z}{r^3} \right] \\
& + \left(\left(\frac{\omega^2 r}{c^2} - \frac{1}{r} \right) \cos(\omega t') + \frac{\omega}{c} \sin(\omega t') \right) x \\
& + \left. \left. \left(\left(\frac{\omega^2 r}{c^2} - \frac{1}{r} \right) \sin(\omega t') - \frac{\omega}{c} \cos(\omega t') \right) y \right] \right) \hat{z} \\
& + \frac{\mu_0 m_0 \omega}{4\pi} \, \frac{1}{r^2} \left[\left(\frac{\omega}{c} \sin(\omega t') - \frac{1}{r} \cos(\omega t') \right) z + \lambda \frac{x}{r} \right. \\
& + \left(\left(\frac{3x}{r^3} - \frac{\omega^2 x}{c^2 r} + \frac{3\omega y}{r^2 c} \right) \cos(\omega t') \right. \\
& + \left. \left. \left(\frac{3y}{r^3} - \frac{\omega^2 y}{c^2 r} - \frac{3\omega x}{r^2 c} \right) \sin(\omega t') + \frac{z}{r^3} \right) xz \right] \hat{x} \\
& + \left[-\left(\frac{1}{r} \sin(\omega t') + \frac{\omega}{c} \cos(\omega t') \right) z + \lambda \frac{y}{r} \right. \\
& + \left(\left(\frac{3x}{r^3} - \frac{\omega^2 x}{c^2 r} + \frac{3\omega y}{r^2 c} \right) \cos(\omega t') \right. \\
& + \left. \left. \left(\frac{3y}{r^3} - \frac{\omega^2 y}{c^2 r} - \frac{3\omega x}{r^2 c} \right) \sin(\omega t') + \frac{z}{r^3} \right) yz \right] \hat{y} \Bigg)
\end{aligned}
$$